



# The structure, function, and biosynthesis of plant cell wall pectic polysaccharides

Kerry Hosmer Caffall<sup>a</sup>, Debra Mohnen<sup>a,b,\*</sup>

<sup>a</sup> University of Georgia, Department of Biochemistry and Molecular Biology and Complex Carbohydrate Research Center, 315 Riverbend Road Athens, GA 30602, United States

<sup>b</sup> DOE BioEnergy Science Center (BESC), 315 Riverbend Road Athens, GA 30602, United States

## ARTICLE INFO

### Article history:

Received 18 November 2008

Received in revised form 4 May 2009

Accepted 6 May 2009

Available online 2 June 2009

### Keywords:

Cell wall polysaccharides

Galacturonan

Glycosyltransferases

Homogalacturonan

Pectin function

Rhamnogalacturonan

## ABSTRACT

Plant cell walls consist of carbohydrate, protein, and aromatic compounds and are essential to the proper growth and development of plants. The carbohydrate components make up ~90% of the primary wall, and are critical to wall function. There is a diversity of polysaccharides that make up the wall and that are classified as one of three types: cellulose, hemicellulose, or pectin. The pectins, which are most abundant in the plant primary cell walls and the middle lamellae, are a class of molecules defined by the presence of galacturonic acid. The pectic polysaccharides include the galacturonans (homogalacturonan, substituted galacturonans, and RG-II) and rhamnogalacturonan-I. Galacturonans have a backbone that consists of  $\alpha$ -1,4-linked galacturonic acid. The identification of glycosyltransferases involved in pectin synthesis is essential to the study of cell wall function in plant growth and development and for maximizing the value and use of plant polysaccharides in industry and human health. A detailed synopsis of the existing literature on pectin structure, function, and biosynthesis is presented.

© 2009 Elsevier Ltd. All rights reserved.

## 1. Introduction

The plant cell wall is a complex macromolecular structure that surrounds and protects the cell, and is a distinguishing characteristic of plants essential to their survival. As a consequence of limited mobility, plants are plastic in their ability to withstand a variety of harsh environmental conditions and to survive attack by pathogens and herbivores. The structure formed by the polysaccharides, proteins, aromatic, and aliphatic compounds of the cell wall enables plants to flourish in diverse environmental niches.

Cell wall structure is continually modified to accommodate the developmental stage and the environmental condition. The plant cell lays down the middle lamella and the primary wall during initial growth and expansion of the cell. In many cells, the wall is thickened and further strengthened by the addition of a secondary wall (Fig. 1). The primary wall is characterized by less relative cellulose and greater pectin compared to secondary walls. The primary wall is thought to contribute to wall structural integrity, cell adhesion, and signal transduction. The major fraction of primary wall non-cellulosic polysaccharides in the Type-I walls of dicot and non-graminaceous species are the pectic polysaccharides. It is the focus of this literature review to bring together the available knowledge of the fine structure, function, and biosynthesis of

the pectic polysaccharides of the plant cell wall, with respect to plant growth and development.

## 2. Pectin structure

The pectic polysaccharides comprise a class of GalA-containing polysaccharides that are abundant in the plant cell wall; comprising as much as 30% of dicot, gymnosperm, and non-Poales monocot walls.<sup>1,2</sup> The walls synthesized by the order Poales (formerly the Gramineae) and related orders contain considerably less pectin; approximately 10% by weight.<sup>3</sup> It has been estimated that ~90% of the uronic acids in the wall derive from the GalpA residues of pectic polysaccharides.<sup>4</sup> The structural classes of the pectic polysaccharides include homogalacturonan (HG), xylogalacturonan (XGA), apiogalacturonan (AGA), rhamnogalacturonan II (RG-II), and rhamnogalacturonan I (RG-I).<sup>1</sup> The fine structure of the pectic polysaccharides governs the biological role(s) of these molecules within the cell wall. Expanding our knowledge of how pectin structure is modified during growth and in response to environmental stimuli is essential to understanding the role of these biological molecules in plant biology.

### 2.1. Homogalacturonan

HG is a polymer of  $\alpha$ -1,4-linked-D-galacturonic acid (Fig. 2) that can account for greater than 60% of pectins in the plant cell wall.<sup>1</sup> HG is abundant in potato (*Solanum tuberosum*) primary walls and,

\* Corresponding author. Tel.: +1 706 542 4458; fax: +1 706 542 4412.

E-mail address: [dmohnen@ccrc.uga.edu](mailto:dmohnen@ccrc.uga.edu) (D. Mohnen).

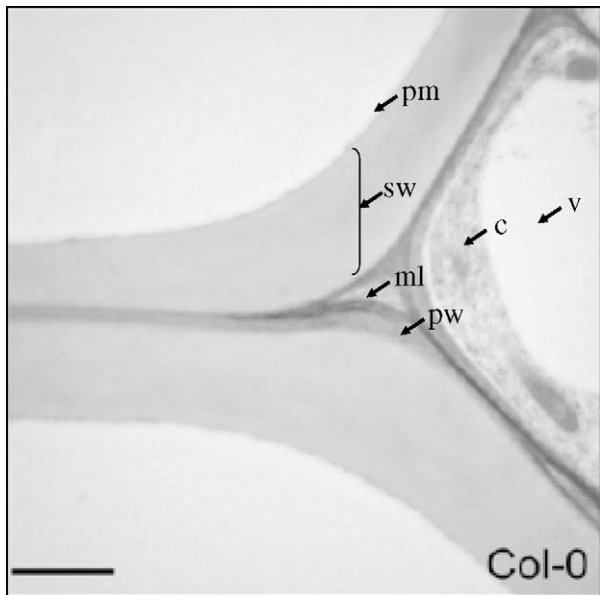


**Figure 1.** The cell wall of *Arabidopsis thaliana*. Transmission electron micrograph of WT *Arabidopsis thaliana* Columbia-0 transverse root section showing the clearly delineated middle lamella (ml), primary wall (pw), and secondary wall (sw) of the metaxylem. Additional labeled features of the cell are the plasma membrane (pm), cytosol (c) and vacuole (v). Bar = 2  $\mu$ M. Adapted from Persson et al. (2007).<sup>291</sup> Copyright American Society of Plant Biologists.

according to immunohistochemical analysis, is particularly dense in the middle lamellae of this species.<sup>5</sup> HG comprises at least 23% of *Arabidopsis thaliana* leaf walls<sup>6</sup> and ~10% of

sycamore suspension culture cell walls (*Acer pseudoplatanus*).<sup>7</sup> The walls of fruits, such as tomato and mango, have up to 35%<sup>8</sup> and ~52% uronic acid,<sup>9</sup> respectively. HG GalpA residues may be methyl-esterified at the C-6 carboxyl or acetylated at the O-2 or O-3 (Fig. 2).<sup>1</sup> The pattern and degree of methylesterification and acetylation varies from source to source. Methylesterification is hypothesized to be tightly regulated by the plant in a developmental and tissue-specific manner.<sup>10</sup> For example, suspension-cultured cotton HG was ~50% methylated with non-random distribution.<sup>11</sup>

The unmethylated C-6 of HG GalA residues is negatively charged and may ionically interact with  $\text{Ca}^{2+}$  to form a stable gel with other pectic molecules if >10 consecutive unmethyl-esterified GalA residues are coordinated.<sup>12</sup> The hypothesized *in vivo* structure of the HG–calcium complex is sometimes referred to as the egg-box model (Fig. 3).<sup>12</sup> The egg-box model describes the close packing of HG that occurs upon  $\text{Ca}^{2+}$ -induced gelling, which accounts for ~70% of the pectic gel in the cell walls of plants.<sup>13</sup> *In vitro*, citrus peel pectin was used to demonstrate that a pectin gel can be formed by addition of salts to pectin de-methylesterified by orange peel pectinmethylesterase (PME). It was postulated that the gel formation was mediated by cations in solution, hydrogen bonding, and hydrophobic interactions.<sup>14</sup> NMR spectroscopy of a calcium pectate gel prepared from orange peel pectin established that the HG backbone has a twofold helical structure ( $2_1$ ), consistent with the egg-box model; however, a small amount of the  $3_1$  helical structure also occurs naturally.<sup>13</sup>

## 2.2. HG is covalently crosslinked to RG-I, RG-II, and possibly other wall polymers

The backbone of HG is covalently linked to RG-I and RG-II, and is also hypothesized to be covalently crosslinked to xyloglucan (XG)

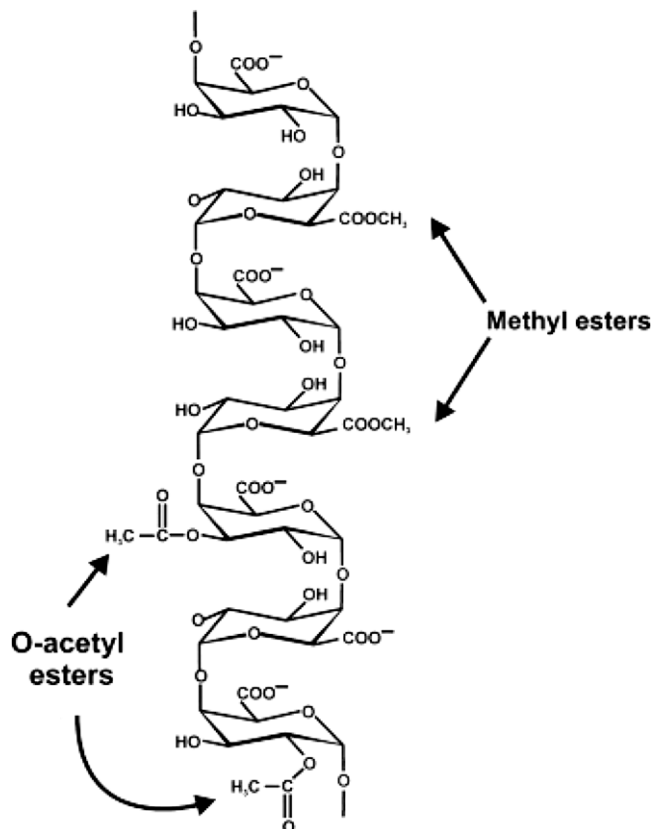


**Figure 2.** Homogalacturonan structure and modification. The structure of the pectic polysaccharide homogalacturonan (HG) as a linear polymer of  $\alpha$ -(1,4)-linked galacturonic acid (GalA) residues. Representative sites of methylesterification at the C-6 and O-acetylation at the O-2 or O-3 of the carbohydrate ring are shown.<sup>1</sup>

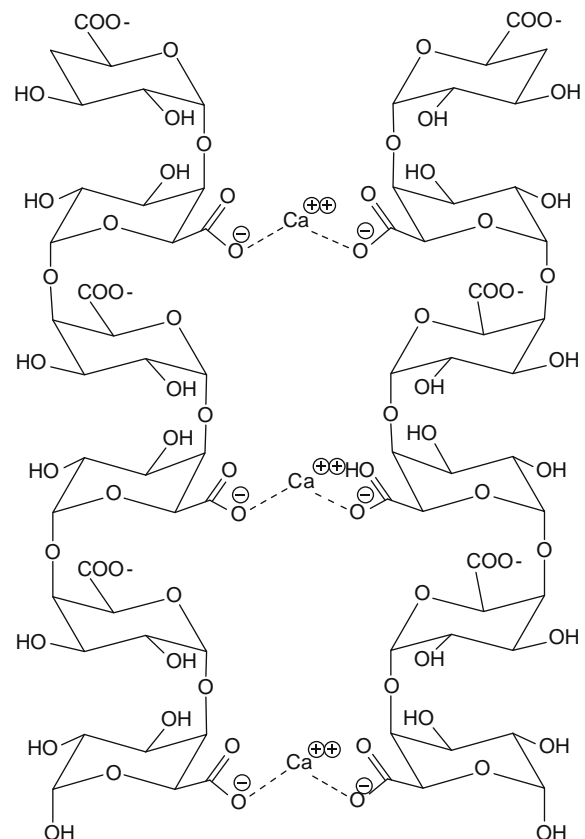


**Figure 3.** The egg-box model of calcium crosslinking in HG polysaccharides.

hemicellulose polysaccharides *in muro*.<sup>15</sup> It has long been observed that pectic polymers are released from wall preparations by endopolygalacturonase (EPG) treatment that hydrolyzes the glycosidic bonds of the HG backbone to produce monomeric, dimeric, or oligomeric fragments.<sup>16</sup> HG, RG-I, and RG-II polysaccharides fail to resolve independently by size exclusion chromatography prior to fragmentation by EPGase digestion.<sup>17,18</sup> In soybean soluble polysaccharides, stretches of  $\alpha$ -(1,4)-linked galacturonic acid were found flanked by RG-I fragments, providing evidence that HG and RG-I are directly and covalently connected through backbone residues.<sup>19</sup> It has also been suggested that HG polysaccharides are linked to xyloglucan based on fragments of XG which were not readily solubilized from walls unless treated with EPG.<sup>7</sup> Further support is provided by discovery of an XG diagnostic fragment, isoprimeverose, that was released from the acidic or pectic fractions of driselase-digested, alkali-extracted walls of *Arabidopsis*, rose, sycamore, tomato, spinach, maize, and barley,<sup>20</sup> suggesting a covalent-crosslink between pectin and a neutral polysaccharide, such as XG.

*In vitro* synthesis of HG with endogenous acceptors yields large polymers with a degree of polymerization (DP) of up to 150 residues<sup>21</sup> that may reflect the size of polysaccharides present *in muro*. The endogenous acceptors in this study, however, were not exhaustively characterized, thus the results reported may represent longer chains than might be found *in muro*. In agreement with the hypothesis of long chain HG in pectin, HG isolated from apple, commercial beet pectin, and commercial citrus pectin were 21,000, 19,000, and 24,000 Da in size, which translates to approximately 72–100 GalA residues in length.<sup>22</sup> Comparable HG domains isolated from dried citrus peel were between 17,000 and 20,600 Da in size,<sup>23</sup> demonstrating that long chain HGs are found in the walls of these species. Reliable sources of EPG of high purity have made

digestion of walls with EPG a popular method of cell wall solubilization, which prevents further characterization of HG domain chain length. The HG intra-RG-I linkers identified in soybean were found to be 4–10 residues in length,<sup>19</sup> fragments much shorter than the previously characterized HG from citrus and beet walls. Because the fragments were isolated from soybean cotyledons, it is unknown if the structure extends to other species or other tissues. The detailed characterization of HG polysaccharide domains and linker structure will aid in the understanding of HG function in plant growth and development.

### 2.3. Substituted galacturonans: apiogalacturonan and xylogalacturonan

The D-apiose-substituted apiogalacturonan (AGA) is found in the walls of aquatic plants such as the duckweeds (*Lemnaceae*)<sup>24</sup> and the marine seagrasses (*Zosteraceae*).<sup>25</sup> Apiose residues are beta-2-linked, 3-linked, as well as 2- and 3-linked to single GalA residues of HG (Fig. 4A). The characterization of AGA by mild extraction of *Lemna* walls showed that the substitution of HG can also occur as apibiose, a disaccharide of apiose (Apif-1,3'-Apif-1-).<sup>2</sup> The level of apiosylation of HG, assessed by the GalA to Api ratio, was observed to be 4 to 1 in *Zosteraceae*, to 4 to 5 in *Lemnaceae*.<sup>24,25</sup> The content of AGA in plant walls appears to fluctuate widely from 0.2% to 20% of non-cellulosic polysaccharides in the dormant buds and the green fronds of giant duckweed, respectively.<sup>26</sup> The abundance of AGA suggests a specifically important structural role in the wall framework of these water-born plants.

Xylogalacturonan (XGA) is HG substituted by D-xylose residues at the C-3 of GalA backbone residues<sup>2,27,28</sup> (Fig. 4B). The characterized XGA in pectic extracts of the *Zosteraceae* marine seagrass consisted of HG substituted by a xylose disaccharide

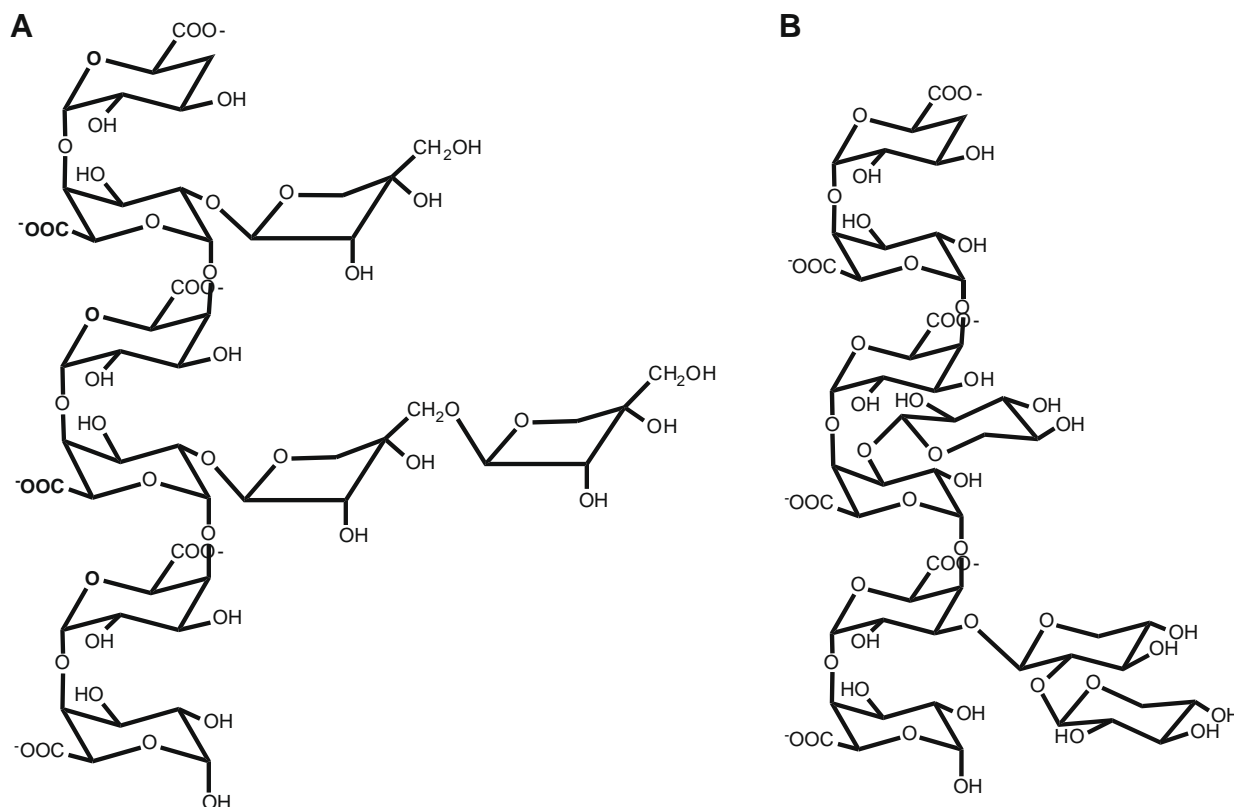


**Figure 4.** The substituted galacturonans xylogalacturonan and apiogalacturonan. Apiogalacturonan (A) is characterized by apiose and 3'-linked apibiose at the 2 position of galacturonan backbone residues. Xylogalacturonan (B) is characterized by xylose and 2-linked xylobiose (not shown) at the 3 position of galacturonan backbone residues.

(Xylp-(1,2)-Xylp-(1,3)-GalpA),<sup>25</sup> while XGA extracted from pea hulls (*Pisum sativum*)<sup>29</sup> was primarily substituted by single xylose residues and only occasionally by an additional 2-linked xylose to form the disaccharide. Results similar to those from pea have been obtained in apple<sup>30</sup> and Arabidopsis,<sup>31</sup> albeit with variation in the extent of xylosylation of the HG. XGA isolated from soybean soluble polysaccharides (*Glycine max*)<sup>28</sup> yielded a fragment of  $\alpha$ -(1,4)-linked GalA residues substituted at the O-3 with chains of approximately one to seven  $\beta$ -(1,4)-linked xylose residues, the first of which is frequently branched at the O-2 by an additional xylose residue. Because the fragment isolated from soybean has not been observed previously in plant cell walls, it is likely to make up a relatively minor component of the wall or to be a structure specific to soybean walls and closely related species. The most abundant XGA polysaccharide structure, which has been observed in multiple species, is the galacturonan backbone substituted at the O-3 by Xyl and by Xyl branched at the O-2 by another Xyl residue.

#### 2.4. Substituted galacturonan: rhamnogalacturonan II

Rhamnogalacturonan II (RG-II) is a substituted galacturonan that is a ubiquitous component of plant walls making up ~4% of suspension-cultured sycamore walls<sup>32</sup> and ~8% of Arabidopsis leaf walls.<sup>6</sup> An RG-II molecule is recognized as a stretch of HG backbone approximately seven to nine residues long with four well-defined side chains, designated A through D (Fig. 5). The structure of RG-II is highly complex with 12 different types of glycosyl residues, including the rare sugar species 2-*O*-methyl xylose, 2-*O*-methyl fucose,<sup>32</sup> aceric acid,<sup>33</sup> 2-keto-3-deoxy-D-lyxo heptulosaric acid (Dha),<sup>34</sup> and 2-keto-3-deoxy-D-manno octulosonic acid (Kdo).<sup>35</sup> Despite its complexity, the conservation of RG-II structure across higher and lower land plants<sup>36</sup> suggests that RG-II must play an important role in wall function.

RG-II molecules are known to self-associate, forming RG-II dimers via a boron diester bond that was first definitively demonstrated by NMR of *in vitro* RG-II-borate complexes derived from sugar beet (*Beta vulgaris*).<sup>37</sup> Early studies showed that boron was an essential microelement in plant growth.<sup>38</sup> The pectic component of walls harbors greater than 60% of total boron content in squash leaves (*Curcubita pepo*) and suspension-cultured tobacco cell walls (*Nicotiana tabacum*).<sup>39</sup> Studies of radish root (*Raphanus sativus*) showed that a single pectic polysaccharide was associated with boron.<sup>40,41</sup> Ultimately, the borate was found to bind the Apif residues of RG-II sidechain A, but not that of sidechain B<sup>37</sup>

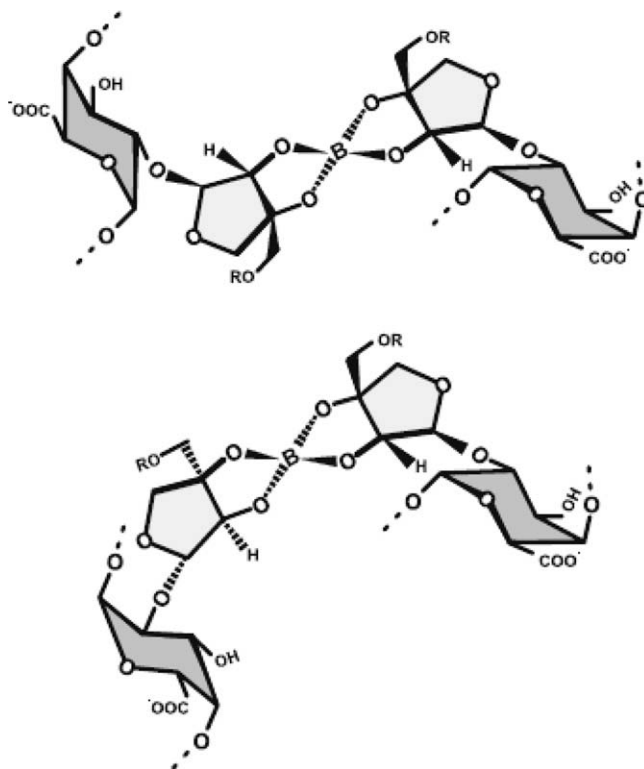


**Figure 6.** The apiosyl residues of rhamnogalacturonan-II sidechain A coordinate boron atoms in the wall. The structure of the two possible isomers of the reversible RG-II-boron diester found in the walls of plants is shown. Adapted with permission from O'Neill and York (2003).

(Fig. 6). The three-dimensional conformation of RG-II sidechain A was found to be mostly stationary in solution, while sidechain B was dynamic. The stationary behavior of sidechain A may provide a binding surface for borate and also contribute directly to the mechanical stability of the RG-II dimer.<sup>42,43</sup>

#### 2.5. Rhamnogalacturonan I

The backbone of the structure of rhamnogalacturonan I (RG-I) has repeating units of  $[\rightarrow\alpha$ -D-GalpA-1,2- $\alpha$ -L-Rhap-1,4 $\rightarrow$ ]<sub>n</sub> as characterized from suspension-cultured sycamore walls (*A. pseudoplat-*

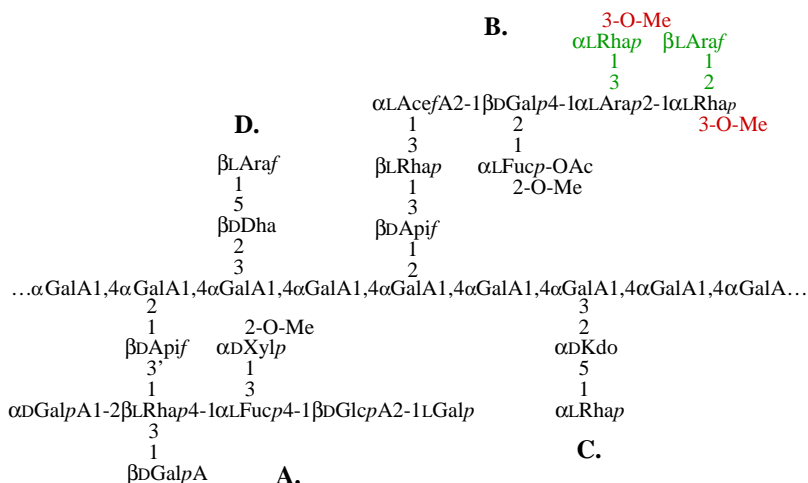


**Figure 5.** The structure of rhamnogalacturonan II found in the walls of land plants. Residues shown in green text are those that are not present in the RG-II of Arabidopsis and closely related species. Modifications shown in red text are those that are present in the RG-II of Pteridophyte and Lycophyte species. Adapted from O'Neill et al. (2004).

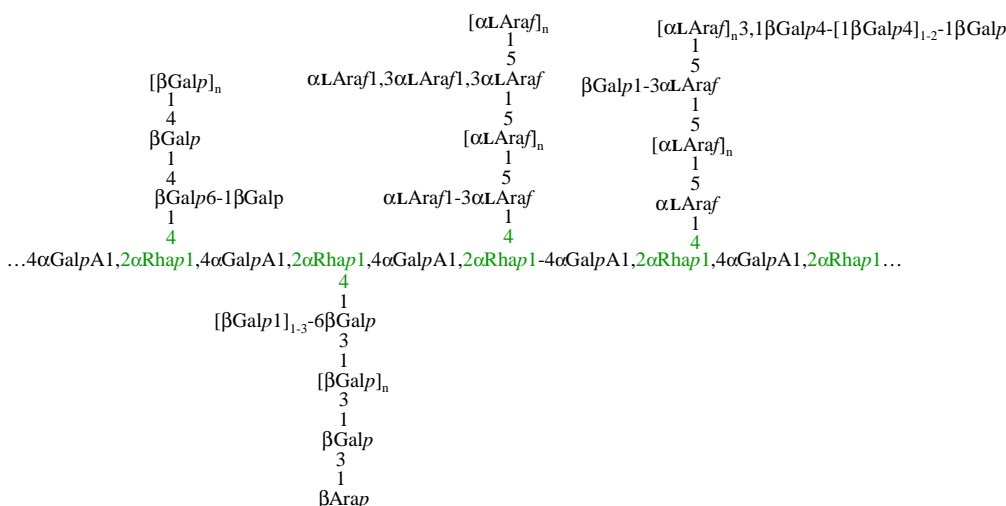


**Figure 7.** The structure of RG-I backbone and representative sidechains. The structure of RG-I with sidechains of  $\alpha$ -(1,5)-l-arabinan,  $\beta$ -(1,4)-galactan, and Type-I arabinogalactan. The  $\alpha$ -1,5-l-arabinan chains that originate from the RG-I backbone may be branched with long chains of 3-linked branches of mono- or di-meric l-arabinan or mono-, di-, or oligomeric branches of  $\beta$ -(1,3)-linked Gal. Type-II arabinogalactan may have branches of 6-linked or 3,6-linked galactose residues. Adapted from O'Neill et al. (2003).

anus<sup>44</sup> and soybean soluble polysaccharides<sup>19</sup> (Fig. 7). Large relative amounts of RG-I are found in the mucilage extruded from the seeds of myxospermous species<sup>45</sup> and in the primary wall and middle lamella of potato (*S. tuberosum*).<sup>5,46,47</sup> Suspension-cultured sycamore walls have ~7% RG-I,<sup>48</sup> while potato tuber walls have ~36% dry weight RG-I polysaccharides.<sup>49</sup> The extended conformation of the RG-I backbone is predicted to take that of a three-fold helix (3<sub>1</sub>).<sup>50</sup> The RG-I isolated from seed mucilage is largely unbranched,<sup>51</sup> while RG-I isolated from walls is branched at approximately half of the rhamnose residues at the C-4 position by arabinan, galactan, or arabinogalactan side chains.<sup>44</sup> The abundance of RG-I sidechains is developmentally and differentially regulated.<sup>5,10,52</sup>

The  $\alpha$ -(1,5)-linked-l-Araf and  $\beta$ -(1,4)-linked-D-Galp chains are 4-linked to approximately half of the rhamnose residues of the RG-I backbone.<sup>53</sup> The RG-I arabinan and galactan side chains from the walls of apple,<sup>54</sup> sugar beet,<sup>55</sup> soybean,<sup>19,56</sup> persimmon,<sup>57</sup> and potato<sup>5,47,49</sup> showed a great deal of heterogeneity in structure from source to source. The RG-I arabinan found in sugar beet and soybean was  $\alpha$ -(1,5)-linked with terminal 3-linked arabinose residues and occasionally with terminal galactose residues.<sup>55,56</sup> However, galactan oligosaccharides have also been found linked to RG-I arabinan, for example, four or more  $\beta$ -(1,4)-linked galactose residues were observed in potato<sup>49</sup> and up to five in soybean.<sup>19</sup>

Three types of galactan polysaccharides have been isolated in association with RG-I polysaccharides: galactan, and Type-I and Type-II arabinogalactan (AG). RG-I galactan from soybean reached 43 to 47  $\beta$ -(1,4)-D-Gal residues in length.<sup>19</sup> Type-I AG is the most abundant RG-I-associated AG. Type-I AG is characterized by single interspersed  $\alpha$ -(1,5)-linked l-Araf residues in a  $\beta$ -(1,4)-linked galactan chain that has branches of one or more Araf residue or single terminal Arap residues.<sup>56</sup> The Type-II AG found in the wall is largely attributed to the post translational modification of arabinogalactan proteins (AGPs), but some Type-II AG in wall preparations is associated with pectic polysaccharides. Type-II AG is characterized by a backbone of  $\beta$ -(1,3)-D-galactan with branch points of 6-linked  $\beta$ -D-Gal of one, two, or three residues in length. Some of the  $\beta$ 1,3-galactan chains are capped by single  $\beta$ -Arap residues.<sup>58</sup>

RG-I may also be modified by single GlcA and 4-O-methyl-GlcA residues, which have been identified in association with RG-I galactan.<sup>59</sup> Wall fragments isolated from acid-hydrolyzed suspension-cultured sycamore RG-I showed single GlcA residues (1,6)-linked and (1,4)-linked to Gal residues, suggesting that these

residues decorate RG-I galactan chains. Thus far, GlcA residues have not been found linked directly to the RG-I backbone<sup>59</sup> and nor have they been found linked to RG-I arabinan.<sup>60</sup>

The complexity of the pectic polysaccharides, and their conservation, to a greater or lesser degree, throughout the plant kingdom, infers specific and important biological functions in the plant cell wall.

### 3. A structural model of the primary cell wall

Current models of the primary plant cell wall structure are based on the hydrogen, covalent and ionic bonding between two or more structural components of the wall. To determine how the many described components of the wall come together as a complete functional wall in vivo is an objective of current cell wall research: how to discern how the matrix polysaccharides of the primary wall function within the framework of the cellulose–xyloglucan structural network? The structure and role of cellulose and hemicellulose in primary walls and the integration of known cellulose, hemicellulose, and pectin structure into a practical three-dimensional model of the primary wall are discussed in the following section.

#### 3.1. Cellulose in primary walls

Cellulose is the foremost load bearing network of the primary and secondary wall. The percentage dry weight of cellulose in a dicot such as Arabidopsis ranges from 15% of leaf<sup>6</sup> to 33% of stem walls.<sup>61</sup> The walls of monocot grass species have approximately 6–10% cellulose in leaves and 20–40% in stems.<sup>62,63</sup> Cellulose is a polymer of  $\beta$ -(1,4)-D-Glc residues that associate with other cellulose chains by hydrogen bonding and Van der Waals forces.<sup>64</sup>

The cellulose chains of plant walls are synthesized at the plasma membrane by cellulose synthase complexes that contain multiple cellulose synthase (CesA) subunits which form a rosette structure. The rosettes consist of 6 globular CesA-containing complexes each of which synthesizes growing cellulose chains of 6–10 cellulose molecules<sup>65,66</sup> which are referred to as 2 nm fibers. Six of the 2-nm fibers then may associate to form microfibrils of approximately 36 glucan chains.<sup>67</sup> The microfibrils average 30 nm in width, a size that may be visualized by spectroscopic methods. The cellulose chains of the primary wall were of low molecular weight compared

to cellulose chains of the secondary wall.<sup>68,69</sup> Cellulose chains may align in parallel (Type I) or antiparallel (Type II)<sup>70</sup> orientation to each other. Only the Type I conformation is known to naturally occur in plants; however, concentrated alkaline treatments may cause Type II cellulose to form during harsh extraction procedures. The cellulose chains may form the Type I $\alpha$  or Type I $\beta$  conformation depending on the extent of staggering of the chains in relation to each other. Type-I $\alpha$  and Type-I $\beta$  are recognized by the triclinic or monoclinic unit cell, respectively, of the crystalline cellulose.<sup>70</sup> The inter-conversion of Type I $\alpha$  and Type I $\beta$  allomers may be induced by mild alkali<sup>70</sup> or by the bending of the cellulose chains,<sup>71</sup> not unlike the reorienting that cellulose microfibrils undergo to run parallel with the surface of the plasma membrane after synthesis. It is also thought that the interaction of cellulose microfibrils with hemicelluloses may affect the ratio of Type I $\alpha$  to Type I $\beta$  cellulose.<sup>71</sup> For example, the developing tracheid of the Japanese hinoki cypress (*Caryota obtusa*) formed greater amounts of the metastable I $\alpha$  in the primary wall, while greater amounts of the stable I $\beta$  were formed in the secondary wall.<sup>72</sup> Primary wall cellulose microfibrils are highly crystalline and oriented parallel to the direction of elongation, contrary to the orientation found in secondary walls.<sup>72</sup> The differences in the size, conformation, crystalline form, degree of crystallinity, and orientation of primary wall cellulose microfibrils are attributed to the stresses that cellulose

microfibrils undergo during rapid cell expansion in the pectinaceous primary wall environment.<sup>69,72</sup>

### 3.2. Hemicellulose

The hemicelluloses are often described as those wall polymers that (1) are solubilized from the wall by alkaline solvents and (2) are  $\beta$ -(1,4)-linked pyranosyl residues that have the O-4 in the equatorial position.<sup>2</sup> These are characteristics that result in a cellulose-like conformation and cause a tendency to hydrogen-bond to cellulose chains. Xylans, mannans, and xyloglucan fit this technical definition, but arabinogalactan is also considered a hemicellulose. The hemicelluloses are more abundant in secondary walls than in the primary walls of both dicots and monocot species. Monocot species have significantly more hemicellulose and less pectin than dicots, and also have mixed linkage glucans that make up a major proportion of monocot hemicellulose polysaccharides.<sup>73</sup>

Xylan polysaccharides comprise linear chains of  $\beta$ -(1,4)-D-Xylp residues and may be found as arabinoxylan (AX), glucuronoarabinoxylan (GAX), glucuronoxyylan (GX), or the unsubstituted homoxylylan (Fig. 8). Xylans also are decorated by acetyl groups at the O-2 or O-3 position.<sup>74</sup> The arabinose residues of AX are primarily terminal residues linked to the 2-position of the xylose backbone in dicots and non-graminaceous species.<sup>3,75</sup> Alternate forms of AX have

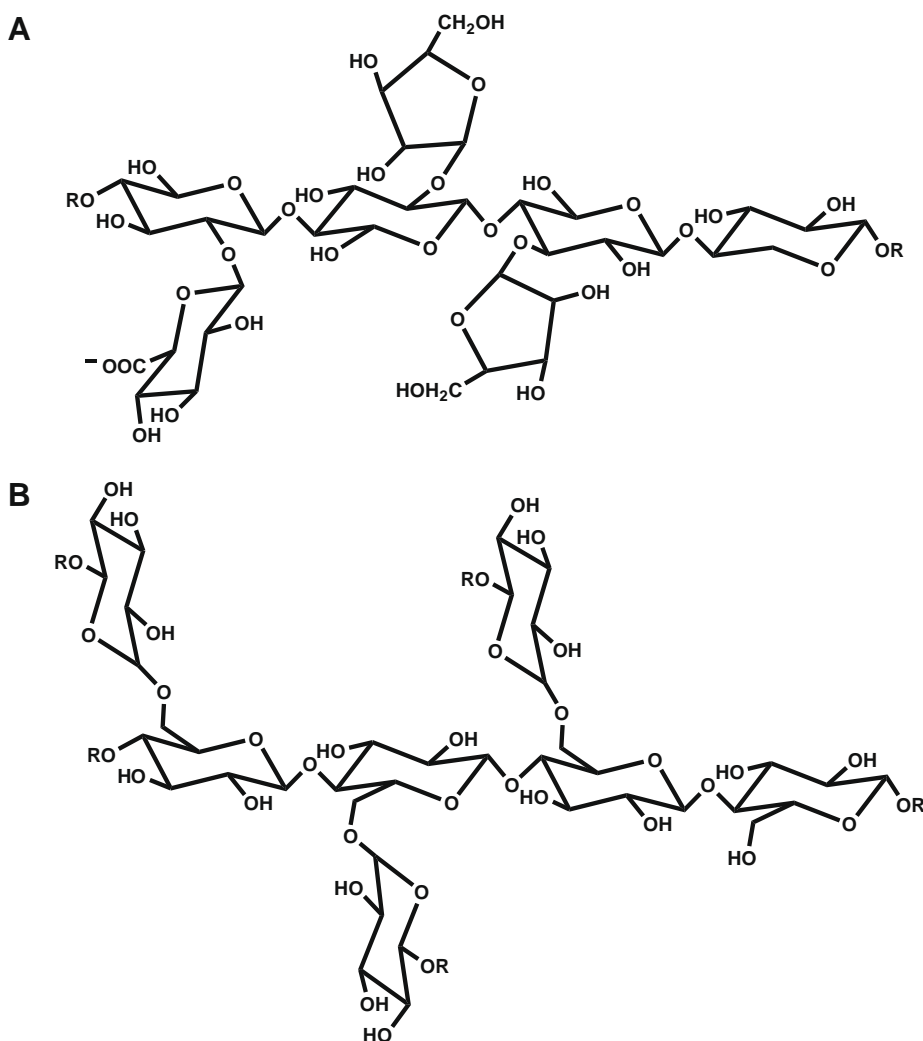


**Figure 8.** The basic structure of xylan and xyloglucan. Glucuronoarabinoxylan (A) is  $\beta$ -(1,4)-D-xylan substituted by glucuronic acid at the O-2 and by arabinose at the O-2 and O-3. Xyloglucan (B) is  $\beta$ -(1,4)-D-glucan, like cellulose, but is substituted at the O-6 by xylose that may be further modified (for known identities of R, see Table 1). The most common pattern of XG backbone substitution is a regular pattern of 3-substituted glucose residues followed by a single free glucose.

been identified in rye wholemeal having arabinose O-2 and O-3 doubly substituted xyloses, substituted arabinoses, terminal xylose, and terminal galactose substitutions.<sup>76</sup> These structures have not, thus far, been confirmed in the primary walls of dicots, suggesting that they are specialized features of cereal walls. AX and GAX are the most abundant xylans in the primary walls of dicots making up ~5% of primary walls of sycamore suspension cultured cells, while AX and GAX constitute ~25% of monocot species.<sup>75</sup> Xylans of higher plants may also be substituted by 4-O-methylglucuronosyl residues.<sup>77</sup> Incorporation of 4-O-methylglucuronic acid to form GX occurs in dicot secondary walls, but is not generally found in the walls of monocots or the primary walls of dicots.<sup>77</sup>

The mannans include the galactomannans (GMs) and the galactoglucomannans (GGMs) that are structurally important components of the cell wall as well as an important source of storage polysaccharides. Mannans have a similar three-dimensional structure to cellulose. Mannans found in some sea weeds of the *Codiaceae* and the *Dasycladaceae* families are known to take the mannan I form, analogous to cellulose I, based on crystallographic methods.<sup>78</sup> In these few unusual species, the mannans form a fibril-like structure 100 Å wide that functionally takes the place of cellulosic fibrils and is the primary structural component in the walls of these sea alga.<sup>78</sup> The specific functions of mannans in the plant cell wall of land plants are unclear, but they appear to play a role in the growth of pollen tubes<sup>79</sup> and roots.<sup>80</sup> While mannan synthase gene expression correlated well with secondary wall synthesis, which is expected for a hemicellulose, mannan synthase genes are also expressed during primary wall synthesis, potentially indicating functional importance of mannans in the structure of the primary wall.<sup>81</sup>

Xyloglucan (XG) is the most abundant hemicellulose in dicot primary walls making up 21% of angiosperm<sup>82</sup> and 10% of gymnosperm suspension-cultured cell walls (*Pseudotsuga menziesii*).<sup>83</sup> The walls of the graminaceous monocots, or grasses, are more than 50% hemicellulosic polysaccharides but only 2–5% of this is xyloglucan.<sup>20,84</sup> Like cellulose, XG has a core backbone structure of  $\beta$ -(1,4)-D-glucopyranose residues; however, XG is heavily decorated with side chains of  $\alpha$ -D-xylose residues linked to the C-6 of backbone glucose residues (Fig. 8). In addition, the structural modification of XG by O-acetylation of backbone Glc residues and sidechain Gal and Fuc or Ara residues has been observed.<sup>85</sup> XG may be hydrolyzed by a XG-specific endoglucanase to yield characteristic oligosaccharides, facilitating structural characterization.<sup>86</sup> The XG structure most frequently found in dicotyledonous flowering plants is that of a repeating heptamer of four Glc residues that have substitutions of  $\alpha$ -D-xylopyranosyl residues at three consecutive Glc backbone residues followed by a single

unsubstituted Glc residue, first isolated from suspension-cultured sycamore cells. Repeating heptamer blocks is considered diagnostic for the presence of XG polysaccharides in dicot species,<sup>82,87</sup> which has not been found in graminaceous monocots that release isoprimeverose, a disaccharide (Xylp- $\alpha$ -(1,6)-Glc), from xyloglucan-specific endoglucanase digestion of grass walls.<sup>88</sup> The XG of graminaceous monocots, instead, consists of 1 or 2 adjacent  $\alpha$ -(1,6)-linked xylosyl residues with ~3 intervening unsubstituted  $\beta$ -(1,4)-linked glucosyl backbone residues.<sup>89</sup> The X substitutions that decorate the  $\beta$ -(1,4)-glucan backbone of XG in dicots are frequently further elongated at the Xyl C-2 by a terminal  $\beta$ -D-Galp (abbreviated L), a disaccharide of  $\alpha$ -L-Fucp-(1,2)- $\beta$ -D-Galp (abbreviated F) or by an increasingly wide variety of less common structural variants (see Table 1). Despite the structural variability found among different species, the functions of XG in plant growth and development are hypothesized to be conserved among all species of flowering plants. XG is thought to primarily function in a structural capacity in the cellulose-xyloglucan network of the plant cell wall, and also has a role in supplying energy stores in the seeds of plants<sup>53,90</sup> and as a signal molecule.<sup>35,88,91</sup> Of relevance to this review is the reported evidence for a linkage between XG and pectins.

The contribution of the cellulose-xyloglucan network to the structural integrity of the plant cell wall has been studied for many years and the subtleties of the interaction of XG, in all of its forms, with cellulose in the primary wall continue to unravel. Strong binding of XG to cellulose has been observed. The strength of the interaction derives from the strong non-covalent and additive interaction of hydrogen bonds between XG molecules and cellulose microfibrils.<sup>18,96</sup> XG is likely to interact with cellulose microfibrils as they are synthesized into the primary wall matrix, causing microfibrils of smaller diameter (less chains per fiber) than those found in secondary walls.<sup>97</sup> The binding of XG to cellulose is also known to weaken cellulose networks,<sup>98</sup> but increases the expansibility of such networks;<sup>99</sup> mechanical properties suited to the expansion and stresses characteristic of conditions during primary wall synthesis.

The XG is bound to cellulose microfibrils in three distinct domains; (1) XG that is endoglucanase accessible, (2) XG that is solubilized by concentrated alkali, and (3) XG that is neither enzyme accessible nor alkali soluble.<sup>100</sup> Molecules of XG have been microscopically visualized to coat and tether the cellulose microfibrils<sup>101,102</sup> and by virtue of the repeating unit structure of XG polysaccharides, bring order to the cellulose network.<sup>103</sup> It has also been observed that XG from different sources (i.e., with distinct populations of the different side chains) binds differently to the cellulose microfibrils.<sup>98</sup> The sidechains of XG modulate the binding

**Table 1**  
The structure and classification of xyloglucan sidechains

Source <sup>a</sup>	Structure of xyloglucan sidechain	Designation <sup>b</sup>	Reference
<i>Acer pseudoplatanus</i>	Glcpc <sup>c</sup>	G	82
<i>Acer pseudoplatanus</i>	T- $\alpha$ -D-Xylp-1,6-Glcpc <sup>c</sup>	X	82
<i>Acer pseudoplatanus</i>	T- $\beta$ -D-Galp-1,2- $\alpha$ -D-Xylp-1,6-Glcpc <sup>c</sup>	L	82
<i>Acer pseudoplatanus</i>	T- $\alpha$ -D-Fucp- $\beta$ -D-Galp-1,2- $\alpha$ -D-Xylp-1,6-Glcpc <sup>c</sup>	F	82
<i>Lycopersicon esculentum</i>	T- $\alpha$ -L-Araf-1,2- $\alpha$ -D-Xylp-1,6-Glcpc <sup>c</sup>	S	93
<i>Lycopersicon esculentum</i>	T- $\beta$ -D-Araf- $\alpha$ -D-Araf- $\alpha$ -1,2- $\alpha$ -D-Xylp-1,6-Glcpc <sup>c</sup>	T	93
<i>Argania spinosa</i>	T- $\beta$ -D-Xylp-1,2- $\alpha$ -D-Xylp-1,6-Glcpc <sup>c</sup>	U	94
<i>Simmondsia chinensis</i>	T- $\alpha$ -L-Galp-1,2- $\beta$ -D-Galp-1,2- $\alpha$ -D-Xylp-1,6-Glcpc <sup>c</sup>	J	95
<i>Acer pseudoplatanus</i>	T- $\alpha$ -L-Araf-1,2-[T- $\alpha$ -D-Xylp-1,6]-Glcpc <sup>c</sup>	A	17
<i>Acer pseudoplatanus</i>	T- $\beta$ -D-Xylp-1,2-[T- $\alpha$ -D-Xylp-1,6]-Glcpc <sup>c</sup>	B	17
<i>Acer pseudoplatanus</i>	T- $\alpha$ -Araf-1,3- $\beta$ -D-Xylp-1,2-[T- $\alpha$ -D-Xylp-1,6]-Glcpc <sup>c</sup>	C	17

Xyloglucan sidechains have variable structure depending on the source of the walls from which the xyloglucan is isolated.

<sup>a</sup> The species from which the xyloglucan was isolated.

<sup>b</sup> A single letter abbreviation used to designate specific XG structures.<sup>92</sup>

<sup>c</sup> T.

of XG to cellulose and thus are important in regulating the mechanical properties of the cellulose–XG network.

### 3.3. The primary cell wall pectic network

The covalent crosslinking of the pectic polysaccharides HG, RG-I, and RG-II has been demonstrated repeatedly in the literature by the EPGase-dependent release of pectic polysaccharides from the wall.<sup>104</sup> The available data suggest that the RG-I and RG-II backbones are continuous with the HG backbone, not that of RG-I sidechains, as suggested by Vincken et al. (2003).<sup>105</sup> If the backbones of the pectins are continuous, the pectic network may be thought of as a macromolecular structure having specific domains of HG, RG-I, and RG-II, however, the arrangement of these domains in vivo is not known. The linkage of HG, RG-I, and RG-II through backbone glycosidic linkages is just one possible way in which the pectins are crosslinked. The pectic network is based on multiple levels of crosslinking that include, but are not limited to, backbone glycosidic linkages, calcium crosslinking, borate ester crosslinking, and covalent linkages to phenolic and possibly other compounds.

The HG domains of pectin may self-associate depending on the degree of methylesterification and thus the affinity of HG for calcium ions. RG-I has a unique backbone of alternating 2-linked Rha and 4-linked GalpA residues. Some rhamnose residues are branched by arabinan, galactan, and/or AG sidechains<sup>48</sup> that may be crosslinked to other wall components such as xylans, xyloglucans, proteins, and lignins. RG-II domains form crosslinks to other RG-II molecules via borate diester linkages, to form RG-II dimers that contribute to wall strength and that affect pore size and flexibility of the pectic network.<sup>37,106</sup> Greater than 95% of RG-II molecules participate in dimer complexes of RG-II.<sup>36</sup> The linkages that pectic polysaccharides make to other pectins, as well as to other wall molecules, combine to assemble the pectic network of the plant cell wall. The complexity of the pectic network structure and the modulation of the pectic crosslinks contribute strength, flexibility, and functionality to the pectic network, and thus, to the primary cell wall.

### 3.4. Pectic crosslinks to hemicelluloses, phenolics, and proteins

There is evidence in the literature to suggest that pectic polysaccharides may also be crosslinked to hemicelluloses, phenolic compounds, and to wall proteins. The crosslinking of pectic polysaccharides to other wall components provides added structural and functional complexity to the wall.

The structure of an oligosaccharide isolated from the mild acid hydrolysates of soy sauce acidic polysaccharides demonstrated what could be a linkage between HG and xylan polysaccharides.<sup>28</sup> In the acidic fraction, ( $\alpha$ -(1,4)-GalpA)<sub>3–4</sub> residues were branched at the C-3 by ( $\beta$ -(1,4)-Xylp)<sub>4–7</sub>. Similar fragments have previously been isolated from soybean cotyledon meal<sup>73</sup> and soy sauce acidic polysaccharide.<sup>107</sup> Because the xylan–HG oligosaccharide fragment has only been identified in soya products, it is unclear whether the xylan–HG crosslink exists in the walls of a subset of species, or whether it is a more common crosslink.

Xyloglucan from the walls of sycamore suspension cells was found to co-chromatograph with neutral sugar-rich acidic polysaccharides.<sup>82</sup> The sycamore xyloglucan/acidic polysaccharide fractions failed to be resolved into separate fractions by endopolygalacturonase treatment alone, but were released only when urea, base, or endoglucanase was applied. Similar phenomena have been observed in kidneybean, rose, tomato, spinach, maize, barley, and Arabidopsis wall fractions.<sup>20,87</sup> Further investigation of this crosslink has suggested that xyloglucan may be linked to the neutral sidechains of RG-I.<sup>18</sup> The anionic component

of *rosa* represented up to ~30% of the total XG<sup>108</sup> and was not separable by HPLC, electrophoresis, 8 M urea, NaOH, or protease treatment. The anionic component and XG was ultimately found to be separable by cellulase, arabinase, galactanase, and endopolygalacturonase treatment, indicating that the anionic component is likely to be RG-I<sup>108</sup>. Walls from Arabidopsis cell cultures pulse-labeled with [<sup>3</sup>H]arabinose were used to further investigate the stage at which XG becomes linked to the anionic pectic polysaccharide.<sup>15</sup> The tritiated XGs were detected within 4 min, which may be too short a time for vesicles to reach the apoplastic space, suggesting that the XG–pectin complex may form during the synthesis of the polysaccharides in the endomembrane system, not after incorporation into the wall. In addition, because the majority of anionic XGs were incorporated into the wall, the XG–pectin complex aids in retention of XG molecules in the wall, preventing their loss to the medium.<sup>15</sup> Based on these analyses, the mechanism of the XG–pectin complex formation is likely to occur in a conserved manner among angiosperms.<sup>20</sup>

Pectin molecules are crosslinked by phenolic compounds that make up >2% of the wall.<sup>2</sup> The most abundant phenolic species found in the walls of Arabidopsis are *para*-coumaryl and feruloyl acids, which present the opportunity for crosslinking, though in most instances this has not been proven. Complexes of feruloylated-xyloglucan and a *p*-coumaroylated-arabinoxylan have been isolated from bamboo shoot walls.<sup>109,110</sup> Feruloylated  $\alpha$ -(1,5)-linked arabinan and  $\beta$ -(1,4)-linked galactan<sup>111</sup> were also isolated from spinach walls. The pulp of spruce and pine wood yielded lignin-carbohydrate  $\beta$ -(1,4)-D-galactan complexes. Interestingly, a small relative amount of arabinose was also found in conjunction with the lignin-carbohydrate complexes, not associated with arabinoxylan based on carbohydrate linkage analysis.<sup>112</sup> As such, the data implicate crosslinking via ferulic and/or *p*-coumaric esters to arabinogalactan,  $\alpha$ -(1,5)-linked arabinan and  $\beta$ -(1,4)-linked galactan in these complexes, which is consistent with the structure of RG-I sidechains.

The structural proteins of the wall make up 2–10% of wall dry weight<sup>2,18</sup> and comprise a variety of wall-associated proteins. The fraction remaining after endopolygalacturonase, endoglucanase, and alkali extraction of sycamore cell walls produced a residue from which further pectic polysaccharides were released only by protease treatment. The release of pectins by protease treatment is likely due to a linkage with the structural protein of the cell wall.<sup>18</sup>

The arabinogalactan proteins (AGPs), proline-rich proteins (PRPs), glycine-rich proteins (GRPs), and wall-associated kinases (WAKs) are wall-associated proteins and are hypothesized to aid in the wall structural reinforcement and regulatory pathways.<sup>84,113</sup> AGPs are highly glycosylated, similar to animal proteoglycan glycoproteins, and are localized to the cell surface by a glycosphatidylinositol-lipid anchor at the plasma membrane.<sup>114</sup> AGPs are typically glycosylated by arabinogalactan sidechains that are 3-linked-D-galactan branched at the C-6 by terminal galactose or arabinose residues (Type I arabinogalactan). Potential signaling and/or structural roles have yet to be determined for each specific AGP. The PRPs are wall-associated proteins that are secreted into the wall matrix wherein they ultimately become crosslinked, conferring strength to the wall.<sup>115</sup> The expression and incorporation of PRPs into the wall can be induced by oxidative bursts that occur during responses to stress,<sup>115</sup> suggesting that these proteins play a role in the defense responses of the plant. The expression of GRPs is also induced by stress.<sup>116</sup> GRPs are hypothesized to interact with components of signaling pathways, and thus, may be regulators of wall structure.<sup>117,118</sup> WAKs have been implicated in cell elongation, morphogenesis,<sup>119,120</sup> and defense against pathogens.<sup>121,122</sup> Undoubtedly, wall-associated proteins serve complex and biological roles with regard to wall structure.



### 3.5. An ultrastructural model of the plant cell wall

Ultrastructural models of the plant cell wall have been formulated based on known cell wall structures in an attempt to integrate available knowledge into a functional structural wall model. The model presented in recent reviews of wall structure argues for two independent networks within the primary cell wall; the pectin–pectin and xyloglucan–cellulose network.<sup>2</sup> In that model, the polysaccharides of the pectic-network, proteins, and phenolic compounds are organized independently around the framework of the cellulose–xyloglucan network. Such a model utilizes the well-established models of the pectin–pectin network and XG–cellulose network. However, there is now well-established evidence to show that a covalent pectin–pectin network exists through the linear backbones of the pectic polysaccharides and that the XG polysaccharides have a strong affinity for cellulose and that XG functions, in part, to coat and tether cellulose microfibrils to form the XG–cellulose networks. Furthermore, there is increasing evidence that pectin interacts, perhaps covalently with hemicellulose such as XG or xylan. Realistic wall models, therefore, must integrate the pectic network, the cellulose xyloglucan network and the available knowledge of other wall structural components that have been characterized. A revised wall model that better takes the current structure data into account, would demonstrate the highly crosslinked wall wherein pectin–pectin, pectin–XG, pectin–phenolics, pectin–protein, and XG–cellulose networks provide a cohesive wall network.<sup>18</sup>

## 4. Function of pectic polysaccharides

The plant cell wall has a functional role in plant growth and development, by contributing to structural integrity, cell adhesion, and mediation of defense responses. The specific roles of pectic polysaccharides in these processes are being elucidated. The plant cell modulates wall structural character in response to growth, differentiation, and environmental stimuli. HG, RG-I, and RG-II are structurally diverse polysaccharides that contribute to primary wall function with regard to cell strength, cell adhesion, stomatal function, and defense response.

### 4.1. HG–calcium complexes contribute to wall strength

Calcium crosslinking of HG contributes to wall strength by bringing blocks of unmethylesterified HG chains into a tightly packed conformation that is dependent on three characteristics: the intramolecular conformation of HG, the charge separation between two GalA molecules in a HG chain, and the efficiency with which HG chains pack together.<sup>123</sup> The extent and pattern of methyl-esterification of HG directly affects the affinity of HG for calcium cations involved in the gelation of HG chains.<sup>14</sup>

A decline in wall expansibility and an increase in wall stiffening have been correlated with a decrease in arabinan and galactan RG-I sidechains and an increase in HG–calcium complexes. In bean pods (*Phaseolus vulgaris*), RG-I neutral sugar sidechains and HG steadily increased during exponential growth and cell expansion. At maturation, the arabinan and galactan were degraded, while the HG continued to accumulate forming HG–calcium complexes.<sup>124</sup> The loss of RG-I sidechains coincided with de-methylation of the pectic component, facilitating HG–calcium complexation. In this study, in addition to tracking the wall polymers at five stages in pea pod development, the enzyme activities of  $\alpha$ -arabinase,  $\beta$ -galactanase, pectinmethyltransferase (PME), polygalacturonase (PG), and peroxidase (POD) were assayed. Dramatic changes in enzyme activity were observed in fully mature (24–55 days after flowering) and senescing (>55 days after flowering) pea pods. The activities of

$\alpha$ -arabinase and  $\beta$ -galactanase and PME gradually increased up to the fully mature stage; thereafter  $\beta$ -galactanase and PME dramatically increased in senescing pods. The data suggest that the loss of RG-I sidechains in combination with the de-methylation of HG, but not the degradation of HG, contributes to the locking of wall components.<sup>124</sup> In soybean, glycerinated hollow cylinders (GHCs) isolated from hypocotyls were used as a tool to study the effect of  $\text{Ca}^{2+}$  on wall tension and wall expansibility.<sup>125</sup> Addition of a calcium chelator to the system dramatically increased wall expansibility, a response that ceased with addition of calcium. The calcium-induced wall stiffening may play a role in decreased wall expansibility and increased strength.<sup>125</sup>

The transgenic expression of EPG in apple, tobacco, and Arabidopsis indicate that HG–calcium complexes likely play a role in wall strengthening and affect wall expansibility. Transgenic plant lines expressing polygalacturonase (PG) have been produced in apple (*Mus domestica*),<sup>126</sup> tobacco, and Arabidopsis,<sup>127</sup> in order to study the changes in wall structure and the developmental abnormalities caused by in vivo pectin degradation. The HG extracted from PG-expressing apple leaf walls was reduced in content and molecular weight. In addition, wall weakening contributed to epidermal tearing of the stomatal guard cells in the apple leaves.<sup>126</sup> Tobacco plants expressing the *Aspergillus niger* endopolygalacturonase-II (AnPG-II) had a dwarfed phenotype and a general weakening of walls that were unable to maintain cell shape and size against the force of turgor pressure.<sup>127</sup>

### 4.2. RG-II borate complexes contribute to wall strength

Boron is hypothesized to function specifically in membrane proteins, plant reproduction, nitrogen fixation, and plant cell wall strengthening.<sup>128</sup> The first definitive proof of a boron requirement in plants was in 1923.<sup>129</sup> A number of reviews have documented the progression of boron research in plant biology through the years.<sup>36,41,130–133</sup> Borate is directly involved in the reversible dimerization of two RG-II molecules that play a critical role in the expansive strength of the plant cell wall and has a specialized role in meristematic and reproductive systems of the plant.

Symptoms of boron deficiency in plants such as slowed root growth, degeneration of new growth, and degeneration of meristematic regions and reproductive organs<sup>128</sup> illustrate the importance of wall borate crosslinking. The Arabidopsis *bor1-1* (high boron requiring) mutant is perpetually boron deficient, and *bor1-1* plants are dwarfed with stems that fail to elongate and have a loss of apical dominance.<sup>134</sup> The Arabidopsis *mur1-1* mutant<sup>135</sup> is morphologically similar to the *bor1-1* mutant, but is deficient in the production of L-fucose, an essential component of RG-II structure caused by a lesion in GDP-mannose-4,6-dehydratase, an enzyme that synthesizes the substrate for addition of fucose into wall polysaccharides; GDP-L-fucose.<sup>136</sup> Normal plants have ~95% of the RG-II molecules in the dimer form, whereas *mur1-1* has only ~50% of RG-II molecules in the dimer form.<sup>136</sup> The L-fucose in sidechains A and B of *mur1-1* RG-II is replaced by L-galactose, but this intriguing in vivo substitution only partially rescues RG-II dimerization in the mutant.<sup>136,137</sup>

The *nolac-H18* mutant (*non-organogenic callus with loosely attached cells*) has a T-DNA insertion in the *NpGUT1* (*N. plumbaginifolia* glucuronosyltransferase 1) gene in tobacco.<sup>138</sup> The *NpGUT1* mutant is deficient in a putative glucuronosyltransferase that has homology to animal exostosin glucuronosyltransferases, and fails to incorporate a GlcA residue, and the corresponding Gal branch [ $\alpha$ -1-Galp-(1,2)- $\beta$ -D-GlcpA-(1,  $\rightarrow$ ), into RG-II sidechain A.<sup>138</sup> The coordination of boron by RG-II is dependent on the specific conformation of RG-II sidechain A, which is compromised in the *mur1-1* and *nolac* mutants.<sup>37,139</sup> The consequence of RG-II-boron complex disruption is a lack of wall expansibility that results in plants that have dwarfed stature, compromised cell adhesion, and defects in

reproductive tissue function.<sup>138,140</sup> The disruption of meristematic regions in *nolac* shoots was similar to that found in boron-deficient pumpkin plants (*Cucurbita moschata*)<sup>138,141</sup> and is hypothesized to be a factor in *nolac* and boron-deficient pumpkin meristematic regions.

#### 4.3. HG–calcium complexes and RG-I sidechains contribute to cell adhesion

Cellular adhesion in plant tissues is mediated by the extracellular matrix or pectic polysaccharides of the plant cell wall. Cell adhesion is reduced in mutants that have insufficient: HG–calcium complexes, branched RG-I polysaccharides, or RG-II dimerization. The colorless non-ripening mutant (*Cnr*), isolated from plantings of commercial tomato (*Lycopersicon esculentum*), grows similar to wild-type fruits up to the mature-green stage, but does not ripen. When wild-type fruits are ripe-red, *Cnr* tomatoes are yellow with white flesh. The mealy texture of *Cnr* tomato flesh<sup>142</sup> and the large intercellular spaces in *Cnr* pericarp compared to WT<sup>143</sup> were an indication of altered cell adhesion.<sup>142</sup> Decreased calcium crosslinking of pectins in the *Cnr* tomato was suggested by increased solubility in water and an overall decrease in chelator soluble pectins, which was confirmed by EELs spectroscopy.<sup>143</sup> The glycosyl residue composition of *Cnr* mature-green walls showed decreases in Rha, Xyl, and uronic acids with increases in galactose compared to WT. Antibody that recognizes a region of unesterified homogalacturonan showed dramatically reduced binding to *Cnr* middle lamellae compared to WT.<sup>143</sup> Interestingly, antibody that binds to  $\alpha$ -(1,5)-arabinan was bound to cytosolic vesicles but not in the walls of *Cnr*, suggesting that arabinan is not being incorporated into the walls of these plants. The changes in cell walls of the *Cnr* tomato mutant correlate with reduced calcium-complexed HG and a lack of wall arabinan incorporation, which implicates these pectic polysaccharides in cell adhesion.

#### 4.4. HG–calcium complexes and RG-I arabinan affect stomatal function

Guard cells were used as a model for cell wall architecture based on the turgor-driven cycle of expansion (opening) and contraction (closing) in stomata that necessitate wall strength as well as expansibility. Epidermal strips (*Commelina communis*) were used to study the changes in stomatal opening in response to wall manipulation by purified wall degrading enzymes.<sup>144</sup> The tremendous turgor pressure that builds up during stomatal opening (up to 5 MPa) causes a volume expansion of each guard cell of up to 70%.<sup>145</sup> Guard cells were induced to open in epidermal peels by fusicoccin and induced to close by ABA, such that normal opening of the stomata was able to be measured and tested after treatment with an assortment of wall degrading enzymes.<sup>144</sup> Surprisingly, only pectinolytic enzymes and a feruloyl esterase had an appreciable affect on pore opening. Degradation of cellulose and hemicellulose by cellulase and xylanase enzymes had no affect on fusicoccin-induced stomatal opening. Endoarabinase, that specifically hydrolyzes  $\alpha$ -(1,5)-l-arabinan, completely blocked pore opening, while feruloyl esterase, FaeA, inhibited but did not stop guard cell pore opening. Open stomata treated with arabinase and induced to close with either ABA or mannitol failed to close, suggesting that the walls were 'locked' into place. Interestingly, a combination of endopolygalacturonase (EPG) and pectinmethyl-esterase (PME) produced much more widely open pores than either treatment alone. The addition of EPG/PME treatment after arabinase-induced wall locking then allowed the stomata to 'unlock' and close. The locking of guard cell walls is also reversed by treatment with strong calcium chelators. Based on these experiments, it is hypothesized that in vivo, the feruloylated RG-I arabinans form ester linkages either to other feruloylated RG-I

arabinans, or to other wall molecules, providing a mechanism for spatial buffering of HG polymers, and thus, by not allowing the HG chains to come into close proximity the HG is inhibited from locking into place by calcium crosslinking (Fig. 9).<sup>144</sup>

#### 4.5. Pectic polysaccharides mediate defense; a barrier and signaling mechanism

The wall provides a physical barrier that pathogens must break down in order to gain entry into the cell to establish infection. Both bacteria and fungal phytopathogenic organisms produce wall hydrolytic enzymes as essential virulence factors that allow entry into plant cells. Wall fragments produced by hydrolytic enzymes may subsequently become signaling molecules to the plant of an impending infection. An early physiological response by the plant may minimize, or end, an attack by phytopathogenic organisms. The action of oligosaccharides as signaling molecules, or oligosaccharins, in plant defense is well documented.<sup>1,146–149</sup> Chitin, chitosan,  $\beta$ -glucan and oligogalacturonides are known to be oligosaccharide elicitors of defense responses.<sup>148</sup> Oligogalacturonides or OGAs, derived from pectic HG, have specialized functions beyond those of structural components in the elicitation of phytoalexins (antibiotic) and reactive oxygen species (ROS).<sup>150,151</sup> Treatment of sodium polypectate or cowpea (*Vigna unguiculata*) walls with PG produced OGAs that were elicitors.<sup>150,152</sup> The elicitor activity was not affected by the specific PG or if the resulting OGA was terminally 4,5-unsaturated, but did depend on an OGA DP of 9–16.<sup>153,154</sup> Phytoalexin elicitor-active OGAs cause changes in gene expression including the induction of genes in a pathway for coumarin phytoalexin biosynthesis, demonstrating that OGA elicitor activity works to induce defense response pathways.<sup>155,156</sup> PG-expressing tobacco plants were also constitutively upregulated in defense responses as a result of wall architectural changes brought about by the fragmentation of HG by PG enzymes.<sup>157</sup>

The action of OGAs is thought to function primarily in defense, but has also been shown to stimulate morphogenesis in specific systems where studied. For example, calcium-dependent induction of flowering shoot growth occurred in tobacco thin-cell layer explants when sycamore-derived OGAs of 12–14 residues in length were applied.<sup>158,159</sup> In addition, specific Arabidopsis apoplastic resident proteins were identified that may be effectors of the biological responses elicited by OGAs.<sup>160</sup> These proteins included a polygalacturonase-inhibiting protein, two lectins, an alpha-glucosidase, an alpha-xylosidase, and a leucine-rich repeat protein. The functions of the specific responses elicited by OGAs, thus, include but are not limited to, defense.

#### 5. Biosynthesis of pectic wall polymers

Pectin biosynthetic glycosyltransferase (GT) enzymes require specific nucleotide-sugar substrates and acceptors for activity. The current model of pectin biosynthesis predicts a Golgi luminal GT active site and nucleotide-sugar substrate, which is thought to be imported into the Golgi lumen by membrane spanning protein transporters or alternatively synthesized within the Golgi lumen.<sup>1,161–164</sup> Here the pertinent historical and progressive research in the synthesis of nucleotide sugars, glycosyltransferases, pectinmethyltransferases, and O-acetyltransferases contributing to the construction of plant cell wall pectic polysaccharides is summarized.

##### 5.1. Subcellular localization of pectin biosynthetic glycosyltransferases

The pectic polysaccharides are synthesized in the Golgi apparatus of the plant cell, sorted to vesicular compartments, and

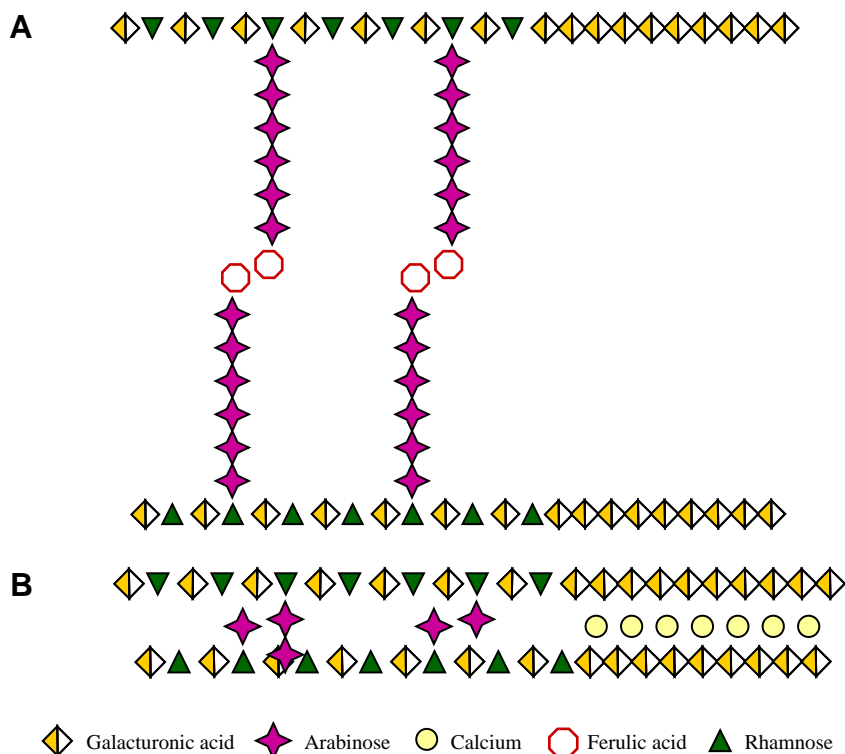


**Figure 9.** The model of arabinan and HG–calcium complexes based on the behavior of stomatal pore openings in response to wall degrading enzymes. The  $\alpha$ -(1,5)-L-arabinan of RG-I may be esterified to ferulic acids that are thought to dimerize providing a linkage between RG-I molecules (A). According to Jones et al. (2003),<sup>144</sup> the arabinan provides a mechanism for the inhibition of HG calcium complexes (yellow/white diamonds (Gala/HG); light yellow circles (calcium), which contribute to wall stiffening (B). Removal of ferulic acid crosslinks by an  $\alpha$ -(1,5)-arabinan-specific endoarabinase or ferulic acid esterase promotes the formation of HG–calcium complexes and wall ‘locking’.<sup>144</sup>

secreted to the apoplastic space.<sup>165</sup> The Golgi apparatus is a complex organelle made up of stacks of flattened vesicles containing proteins geared to the sorting and processing of cargo in specific Golgi vesicles. A Golgi stack has four defined regions; the cis, medial, trans Golgi, and the trans-Golgi network<sup>166</sup> (Fig. 10). Cargo intended for secretion is transported through the endoplasmic reticulum (ER) to the cis face of the Golgi body. Wall polysaccharides are continually synthesized and moved through Golgi stacks from the cis face to the trans face of the Golgi where they are sorted and packaged into the vesicles of the trans-Golgi network (TGN) for transport to the plasma membrane, the cell plate of dividing cells or the vacuole.<sup>167</sup>

In plants, transport from the ER to the Golgi may occur via clathrin coated COPII vesicles or by direct connections that physically link ER and Golgi membranes. Movement through the Golgi is thought to occur via two complementary mechanisms as described by the vesicle shuttle model and the cisternae maturation model.<sup>168</sup> The vesicle shuttle model proposes that each cisterna is stable and functionally specific, while the cargo is transported stack to stack by vesicular shuttles. The cisternae maturation model proposes that the resident processing enzymes may be regulated by retrograde transport of enzymes in COPI vesicles while cargo is moved in bulk within the cisternae; from cis to trans Golgi.<sup>169</sup> Transport in the secretory system is known to involve a host of proteins that regulate and orchestrate the initiation, formation, and direction of secretory vesicle movement associated with the Golgi. Vesicle trafficking in the Golgi is a complex process for which there are many valuable reviews.<sup>168,170–174</sup>

The synthesis of polysaccharides in the Golgi and their movement to the plasma membrane have been tracked by histochemical analysis of plant cells. Antibody probes that recognize epitopes of carrot extensin-1, sycamore deesterified RG-I/HG, and purified syc-

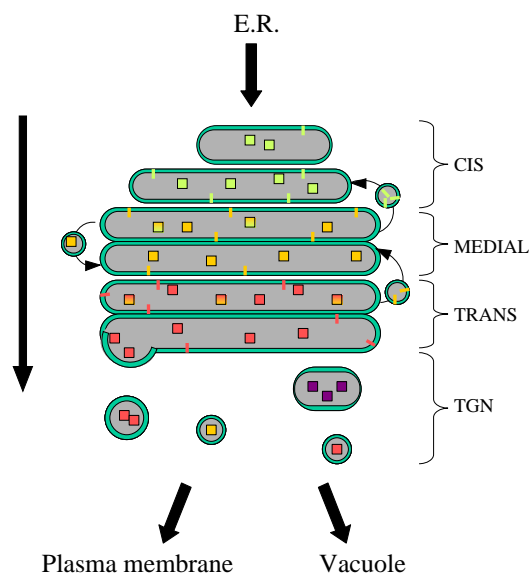


**Figure 10.** The plant Golgi apparatus. Each Golgi apparatus is composed of flattened vesicles within which glycoproteins and wall polysaccharides (cargo-colored squares) are synthesized largely by membrane bound glycosyltransferases (colored sticks). The direction of cargo flow is depicted by the large black arrows. The Golgi cargo is received from the endoplasmic reticulum (ER) at the cis-face of the Golgi and traverses to the medial, trans, and the trans-Golgi network (TGN) for further processing and export.

amore XG had differential binding to specific Golgi stacks. RG-I epitopes appeared in the cis and medial Golgi and the XG epitopes were present in the medial, trans, and TGN, while the extensin

epitopes were observed throughout the Golgi.<sup>165,175</sup> The spatially distinct localization of these Golgi products demonstrated that glycoproteins and wall polysaccharides are both simultaneously synthesized in the Golgi, but appear to have different sorting and export programs.<sup>175</sup> The differential localization of RG-I, XG, and extension epitopes also suggest the separation of glycoprotein, as well as acidic and neutral polysaccharide biosynthetic machinery, within the Golgi apparatus.

The localization of pectic polysaccharide epitopes within the cisternae of the Golgi sets the stage for biochemical localization of the activities necessary for pectin biosynthesis. Multiple activities are necessary for the synthesis of HG, RG-I, and RG-II (Table 2) and many glycosyltransferases are required for the complete synthesis of pectic polysaccharides.<sup>163,164,176</sup> The subcellular localization of pectin biosynthetic HG:α1,4-GalAT,<sup>177</sup> RG-I:β1,4-GalT,<sup>178</sup> and α1,5-AraT<sup>179</sup> has been investigated. HG:GalAT activity was detected exclusively in Golgi-enriched fractions based on the correlation with latent UDPase activity, a Golgi-resident activity.<sup>177</sup> Pea homogenates (*P. sativum*) were subjected to discontinuous sucrose density gradient, which separates membrane fractions derived from ER, Golgi, and the plasma membrane according to relative density. Proteinase K treatment of GalAT activity-positive Golgi fractions, with and without dissolution of membranes by Triton X-100 detergent, demonstrated that GalAT activity is preserved in the presence of Proteinase K without Triton X-100 but is lost after addition of detergent, a situation that can exist only if the active site of the HG:GalAT is located in the lumen of the Golgi, and thus is protected from Proteinase K degradation.<sup>177</sup> Pectin biosynthetic β1,4-GalT activity in potato stems (*S. tuberosum*)<sup>178</sup> and arabinosyltransferase (AraT) activity in mung bean (*Vigna radiata*)<sup>179</sup> were also localized specifically to the Golgi, suggesting that the pectin biosynthetic machinery is likely located within the Golgi apparatus.

## 5.2. Nucleotide-sugar interconverting enzymes in pectin biosynthesis

Diverse biosynthetic pathways lead to the synthesis of the specific nucleotide-sugars required for plant pectin biosynthesis (Fig. 11). Progress has been rapid in the elucidation of the *A. thaliana* nucleotide-sugar interconverting pathways due to the completion of the Arabidopsis genome sequence.<sup>194</sup> Nucleotide-sugars may be formed via salvage pathways from sugars recycled from the wall polysaccharides or from sugars supplied to cultured cells.<sup>195,196</sup> Such nucleotide-sugars, or primary sugar phosphates derived directly from photosynthesis metabolism, are converted into a diverse array of sugar donor molecules by the nucleotide-sugar interconverting enzymes (NIEs) (Table 3). For this discussion, the advances in Arabidopsis NIE discovery will be covered as a means to condense the material currently existing in the literature in reference to plant and bacterial NIEs. Nucleotide-sugars are substrates for the enzyme-catalyzed transfer of a sugar group to an acceptor molecule in polysaccharide biosynthesis. If the appropriate nucleotide-sugar is not synthesized in the plant, synthesis is hindered. Nucleotide-sugars are supplied to wall biosynthetic glycosyltransferases by NIEs that regulate wall polysaccharide biosynthesis and are themselves frequently regulated by elements of the NIE pathway.<sup>203,206</sup> Evidence of NIE regulation of nucleotide-sugar availability is observed in the biological shift from primary wall to secondary wall synthesis: the abundance of nucleotide-sugars and their precursors is coordinately shifted to reflect an up-regulation in hemicellulose and cellulose nucleotide-sugar substrates and a down-regulation in pectic polysaccharide nucleotide-sugar substrates.<sup>198</sup> Arabidopsis mutants have been isolated that demonstrate the role of NIEs in pectin biosynthesis. The nucleotide-sugar interconverting pathway mutant, *mur1*, showed disrupted RG-II

synthesis, stemming from a lesion in a GDP-D-mannose-4,6-dehydrogenase gene (GMD1). GMD1 is a key component in the synthesis of GDP-fucose that is necessary for the correct synthesis of cell wall RG-II and of fucosylated xyloglucans. UDP-D-4-glucose epimerase (UGE) catalyzes the epimerization of UDP-D-Glc to UDP-D-Gal, which has an effect on the specific incorporation of Gal onto XG sidechains, Type-II arabinogalactan (β-1,6-galactan) and to a lesser extent RG-I.<sup>201</sup> The Arabidopsis root hair deficient mutants (*rhd 1-1*, *reb1-1/rhd1-2*, *reb1-2/rhd1-3*, and *rhd1-4*) are deficient in UGE4, lack root hairs, and show weakened swollen walls of root trichoblast cells.<sup>202,224–226</sup> Monoclonal antibodies specific to fucosylated XG (CCRC M1) and fucosylated AGPs (CCRC M7) showed an absence of CCRC M1 label in *rhd* root sections and a clear reduction in CCRC-M7 label.<sup>201</sup> In addition, binding of the AGP-specific monoclonal antibodies, JIM14 and LM2, was reduced in trichoblast cells, indicating that the specific and dramatic alterations were brought about by a mutation in the NIE UGE4.<sup>202</sup>

Evidence for NIE involvement in, and regulation of, wall biosynthesis is provided by biochemical and kinetic data on the activities of specific NIEs that are themselves regulated by components of the nucleotide-sugar interconversion pathway.<sup>197,203</sup> UDP-D-Xyl is synthesized by the decarboxylation of UDP-D-GlcA by UDP-D-Xyl synthase (UXS), and UDP-D-Xyl is in turn utilized for the synthesis of UDP-D-Ara.<sup>209</sup> Representatives of the UXS gene family were expressed in *Escherichia coli*.<sup>209</sup> The product of UXS (UDP-Xyl) down-regulates upstream components of the nucleotide-sugar interconverting pathway by negative feedback: UDP-Glc dehydrogenase and UDP-Glc pyrophosphorylase are strongly inhibited by UDP-Xyl.<sup>208</sup> The activity of UXS is itself down-regulated by UDP-Xyl, UMP, UDP, and UTP.<sup>209</sup> The activity of an additional NIE is also regulated by other products of the nucleotide-sugar interconverting pathway. The UDP-Api/UDP-Xyl synthase (AXS) synthesizes UDP-Api or UDP-Xyl from UDP-GlcA, depending on reaction conditions. AXS activity is inhibited by UDP-GalA by as much as 69%.<sup>212</sup> It is proposed that UDP-GalA is a regulator of AXS in vivo.<sup>212</sup> Rhamnose biosynthesis (RHM) is responsible for the synthesis of UDP-L-Rha from UDP-D-Glc by three distinct activities; UDP-D-glucose-4,6-dehydratase, UDP-4-keto-6-deoxy-D-glucose-3,5-epimerase, and UDP-4-keto-L-rhamnose 4-keto-reductase.<sup>211</sup> The activity of RHM is inhibited by UDP-Rha, UDP-Xyl, and UMP, and thus, the levels of UDP-Glc and UDP-Rha in the cell are regulated by the concentrations of these nucleotide-sugars.<sup>211</sup> Regulation of NIEs in plant cells by negative feedback inhibition provides a mechanism for control of wall polysaccharide biosynthesis.<sup>227</sup>

## 5.3. HG glycosyltransferases

The HG backbone is a polymer of α1,4-linked GalA residues and is proposed to require several α1,4-GalATs (HG:GalATs) to synthesize the entire complement of HG required throughout plant development (Table 2). HG:GalATs specifically catalyze the transfer of D-GalA from UDP-D-GalA onto a growing stretch of HG (E.C. 2.4.1.43) via a lumenally facing HG:GalAT catalytic domain.<sup>177</sup> GAUT1, the only functionally proven HG:GalAT, has been shown to be Golgi localized, and the other GAUT1-related gene family members are also predicted to be Golgi-localized Type-II membrane proteins.<sup>228</sup> The activity of plant HG:GalAT was first critically evaluated in pea.<sup>229</sup> Unmethylated UDP-D-GalA was the preferred nucleotide-sugar substrate for elongation of endogenous acceptors in particulate membrane fractions of mung bean (*V. radiata*).<sup>229</sup> HG:GalAT activity has also been characterized in tomato (*L. esculentum*), turnip (*Brassica rapa*),<sup>230,238</sup> tobacco (*N. tabacum*),<sup>232</sup> azuki bean (*Vigna angularis*),<sup>234</sup> pea (*P. sativum*),<sup>177</sup> petunia (*Petunia axillaris*),<sup>235</sup> pumpkin (*C. moschata*),<sup>236</sup> and Arabidopsis (*A. thaliana*).<sup>228,292</sup>

The solubilized HG:GalAT activity from tobacco microsomal membrane particulate preparations catalyzed the transfer of GalA

**Table 2**  
Predicted glycosyltransferases required for pectin biosynthesis<sup>a,b</sup>

Glycosyltransferase	Parent polymer	Enzyme acceptor	Structure reference
<i>HG glycosyltransferases</i>			
$\alpha$ -1,4-GalAT <sup>c</sup>	HG/RG-II	D-GalpA- $\alpha$ -(1→4)-D-GalpA- $\alpha$ -(1→	180
<i>RG-I glycosyltransferases</i>			
$\alpha$ -(1,2)-GalAT	RG-I	L-Rhap- $\alpha$ -(1→4)-D-GalpA- $\alpha$ -(1→	48,44,180
$\alpha$ -(1,4)-GalAT	RG-I/HG	D-GalpA- $\alpha$ -(1→2)-L-Rhap- $\alpha$ -(1→	19
$\alpha$ -(1,4)-GalAT	RG-I/HG	D-Xylp-?	181,28
$\alpha$ -(1,4)-RhaT	RG-I	D-GalpA- $\alpha$ -(1→2)-L-Rhap- $\alpha$ -(1→	48,44,180
$\alpha$ -(1,4)-RhaT	HG/RG-I	D-GalpA- $\alpha$ -(1→4)-D-GalpA- $\alpha$ -(1→	19
$\beta$ -(1,4)-GalIT	RG-I	L-Rhap- $\alpha$ -(1→4)-D-GalpA- $\alpha$ -(1→	182,180,30
$\beta$ -(1,4)-GalIT	RG-I	D-Galp- $\beta$ -(1→4)-L-Rhap- $\alpha$ -(1→	182,180
$\beta$ -(1,4)-GalIT	RG-I	D-Galp- $\beta$ -(1→4)-D-Galp- $\beta$ -(1→	73,183,182,180,19
$\beta$ -(1,6)-GalIT	RG-I	D-Galp- $\beta$ -(1→4)-D-Galp- $\beta$ -(1→	182,180,184
$\beta$ -(1,3)-GalIT	RG-I/AGP	D-Galp- $\beta$ -(1→3)-D-Galp- $\beta$ -(1→	180,53
$\beta$ -(1,6)-GalIT	RG-I/AGP	D-Galp- $\beta$ -(1→3)-D-Galp- $\beta$ -(1→	180,53
$\beta$ -(1,6)-GalIT	RG-I/AGP	D-Galp- $\beta$ -(1→6)-D-Galp- $\beta$ -(1→3)-D-Galp- $\beta$ -(1→	180,53
(1,5)-GalIT	RG-I	L-Araf- $\alpha$ -(1→4)-D-Galp- $\beta$ -(1→	56
$\alpha$ -(1,4)-ArafT	RG-I	L-Rhap- $\alpha$ -(1→4)-D-GalpA- $\alpha$ -(1→	182
$\alpha$ -(1,5)-ArafT	RG-I	L-Araf- $\alpha$ -(1→5)-L-Araf- $\alpha$ -(1→	60
$\alpha$ -(1,5)-ArafT	RG-I	D-Galp- $\beta$ -(1→4)-D-Galp- $\beta$ -(1→	56
$\alpha$ -(1,3)-ArafT	RG-I	D-Galp- $\beta$ -(1→4)-L-Rhap- $\alpha$ -(1→	182,180
$\alpha$ -(1,2)-ArafT	RG-I	L-Araf- $\alpha$ -(1→3)-D-Galp- $\beta$ -(1→	182,180
$\alpha$ -(1,5)-ArafT	RG-I	L-Araf- $\alpha$ -(1→2)-L-Araf- $\alpha$ -(1→	182,180
$\alpha$ -(1,3)-ArafT	RG-I	L-Araf- $\alpha$ -(1→5)-L-Araf- $\alpha$ -(1→	53
$\alpha$ -(1,2)-ArafT	RG-I	L-Araf- $\alpha$ -(1→5)-L-Araf- $\alpha$ -(1→	53
$\alpha$ -(1,3)-ArafT	RG-I	L-Araf- $\alpha$ -(1→3)-L-Araf- $\alpha$ -(1→	53
$\alpha$ -(1,5)-ArafT	RG-I	L-Araf- $\alpha$ -(1→3)-L-Araf- $\alpha$ -(1→	53
$\alpha$ -(1,3)-ArafT	RG-I	D-Galp- $\beta$ -(1→4)-D-Galp- $\beta$ -(1→	73,183,185
(1,5)-ArafT	RG-I	L-Araf- $\alpha$ -(1→3)-D-Galp- $\beta$ -(1→	73,183
$\alpha$ -(1,6)-ArafT	RG-I	D-Galp- $\beta$ -(1→4)-D-Galp- $\beta$ -(1→	184
$\alpha$ -(1,4)-ArafT	RG-I	D-Galp- $\beta$ -(1→4)-D-Galp- $\beta$ -(1→	56
$\alpha$ -(1,4)-ArapT	RG-I	D-Galp- $\beta$ -(1→4)-D-Galp- $\beta$ -(1→	184
$\beta$ -(1,3)-ArapT	RG-I	L-Araf- $\alpha$ -(1→5)-L-Araf- $\alpha$ -(1→	186
$\alpha$ -(1,3)-ArafT	RG-I/AGP	D-Galp- $\beta$ -(1→6)-D-Galp- $\beta$ -(1→	53
$\alpha$ -(1,6)-ArafT	RG-I/AGP	D-Galp- $\beta$ -(1→6)-D-Galp- $\beta$ -(1→	53
$\alpha$ -(1,2)-FucT	RG-I	D-Galp- $\beta$ -(1→4)-D-Galp- $\beta$ -(1→	182,180
$\beta$ -(1,4)-GlcAT	RG-I	Gal-?	59
$\beta$ -(1,6)-GlcAT	RG-I	Gal-?	59
$\beta$ -(1,4)-XylIT	RG-I	L-Rhap- $\alpha$ -(1,4)-D-GalpA- $\alpha$ -(→	57,187
$\beta$ -(1,4)-XylIT	RG-I	D-Xylp- $\beta$ -(1,4)-L-Rhap- $\alpha$ -(1,4)-D-GalpA- $\alpha$ -(→	187
<i>XGA glycosyltransferases</i>			
$\beta$ -(1,3)-XylIT	XGA	D-GalpA- $\alpha$ -(1→4)-D-GalpA- $\alpha$ -(1→	27,107,188,28
$\beta$ -(1,2)-XylIT	XGA	D-Xylp-(1→3)-D-GalpA- $\alpha$ -(1→	25
$\beta$ -(1,4)-XylIT	XGA	D-Xylp- $\beta$ -(1→3)-D-GalpA- $\alpha$ -(1→	28
$\beta$ -(1,2)-XylIT	XGA	D-Xylp-(1→4)-D-Xylp-(1→3)-D-GalpA- $\alpha$ -(1→	28
$\beta$ -(1,4)-XylIT	XGA	D-Xylp- $\beta$ -(1→4)-D-Xylp- $\beta$ -(1→3)-GalpA-(1→	28
<i>AGA glycosyltransferases</i>			
$\beta$ -(1,2)-ApiT	AGA	D-GalpA- $\alpha$ -(1→4)-D-GalpA- $\alpha$ -(1→	189,190
$\beta$ -(1,3)-ApiT	AGA	D-GalpA- $\alpha$ -(1→4)-D-GalpA- $\alpha$ -(1→	189,190
$\beta$ -(1,3)-ApiT	AGA	D-Apif- $\beta$ -(1→2)-D-GalpA- $\alpha$ -(1→	189,190
$\beta$ -(1,3)-ApiT	AGA	D-Apif- $\beta$ -(1→3)-D-GalpA- $\alpha$ -(1→	189,190
<i>RG-II glycosyltransferases</i>			
$\alpha$ -(1,2)-GalAT	RG-II-A	L-Rhap- $\beta$ -(1→3')-D-Apif-(1→	83,191,137
$\beta$ -(1,3)-GalAT	RG-II-A	L-Rhap- $\beta$ -(1→3')-D-Apif-(1→	83,191,137
$\beta$ -(1,3')-RhaT	RG-II-A/B	D-Apif- $\beta$ -(1→2)-D-GalpA- $\alpha$ -(1→	83,191,137
$\alpha$ -(1,3)-RhaT	RG-II-B	L-Arap- $\alpha$ -(1→4)-D-Galp- $\beta$ -(1→	83,192,193,137
$\alpha$ -(1,2)-RhaT	RG-II-B	L-Arap- $\alpha$ -(1→4)-D-Galp- $\beta$ -(1→	192,137
$\alpha$ -(1,5)-RhaT	RG-II-C	D-Kdop- $\alpha$ -(2→3)-D-GalpA- $\alpha$ -(1→	35,137
$\alpha$ -(1,2)-L-GalIT	RG-II-A	D-GlcpA- $\beta$ -(1→4)-L-Fucp- $\alpha$ -(1→	35,83,137
$\beta$ -(1,2)-GalIT	RG-II-B	L-AcefA- $\alpha$ -(1→3)-L-Rhap- $\beta$ -(1→	83,191,137
$\alpha$ -(1,4)-ArapT	RG-II-B	D-Galp- $\beta$ -(1→2)-L-AcefA- $\alpha$ -(1→	83,191,137
$\beta$ -(1,2)-ArafT	RG-II-B	L-Rhap- $\alpha$ -(1→2)-L-Arap- $\alpha$ -(1→	192,137
$\beta$ -(1,5)-ArafT	RG-II-D	D-Dhap- $\beta$ -(2→3)-D-GalpA- $\alpha$ -(1→	34,191,137
$\alpha$ -(1,4)-L-FucT	RG-II-A	L-Rhap- $\beta$ -(1→3')-D-Apif- $\beta$ -(1→	83,137
$\alpha$ -(1,2)-L-FucT	RG-II-B	D-Galp- $\beta$ -(1→2)-L-AcefA- $\alpha$ -(1→	83,191,137
$\beta$ -(1,2)-ApiT	RG-II-A/B	D-GalpA- $\alpha$ -(1→4)-D-GalpA- $\alpha$ -(1→	83,191,137
$\alpha$ -(1,3)-XylIT	RG-II-A	L-Fucp- $\alpha$ -(1→4)-L-Rhap- $\beta$ -(1→	83,137
$\beta$ -(1,4)-GlcAT	RG-II-A	L-Fucp- $\alpha$ -(1→4)-L-Rhap- $\beta$ -(1→	83,138,137
$\alpha$ -(2,3)-KdoT	RG-II-C	D-GalpA- $\alpha$ -(1→4)-D-GalpA- $\alpha$ -(1→	35,137
$\beta$ -(2,3)-DhaT	RG-II-D	D-GalpA- $\alpha$ -(1→4)-D-GalpA- $\alpha$ -(1→	34,191,137
$\alpha$ -(1,3)-AceA/T	RG-II-B	L-Rhap- $\beta$ -(1→3')-D-Apif- $\beta$ -(1→	83,191,137

?: unknown anomeric configuration or attached glycosyl residue.

<sup>a</sup> Adapted from Mohnen (2002),<sup>265</sup> Mohnen et al. (2008),<sup>164</sup> and Sterling Ph.D. dissertation (2004).<sup>b</sup> The glycosyltransferases necessary for the synthesis of homogalacturonan (HG), rhamnogalacturonan-I (RG-I), xylogalacturonan (XGA), apiogalacturonan (AGA), and rhamnogalacturonan-II (RG-II) are listed based on the current understanding of pectic polysaccharide structure according to the corresponding structure references.<sup>c</sup> Multiple GalATs for synthesis of HG, XGA, AGA, and RG-II.

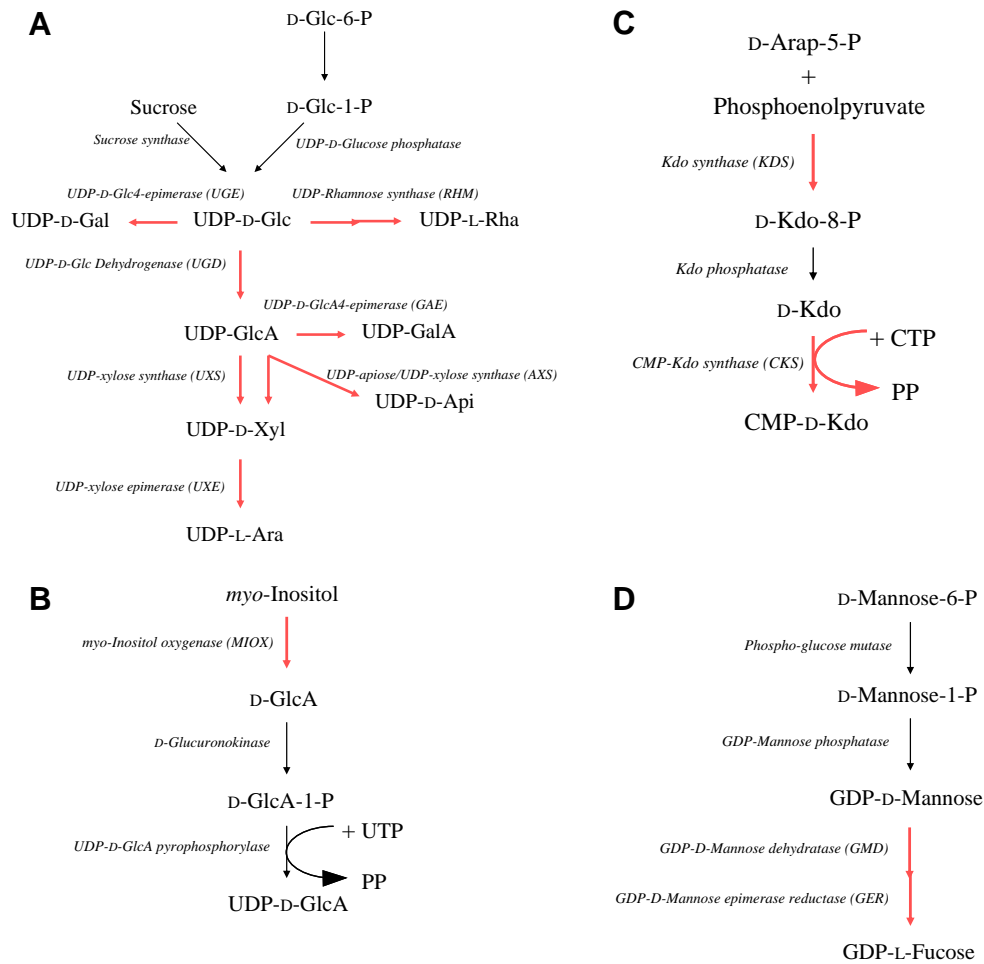


**Figure 11.** The plant nucleotide-sugar interconverting pathways. Species of nucleotide-sugars created from UDP-D-Glc (A) and myo-inositol (B) in an alternate pathway. The proposed mechanism of plant CMP-D-Kdo (C) and GDP-L-Fuc synthesis (D).

from UDP-D-GalA preferentially to the non-reducing end of OGA acceptors of DP 10 or greater.<sup>21,239</sup> The products formed were of an  $\alpha$ -(1,4)-configuration as demonstrated by the endo- or exopolylgalacturonase degradation of the reaction products to yield GalA.<sup>21</sup> The tobacco-solubilized enzyme, under the low relative UDP-GalA conditions used, added only single GalA residues in a non-processive manner.<sup>21</sup> However, the pumpkin detergent-permeabilized GalAT activity, under higher relative UDP-GalA concentrations, catalyzed the addition of up to 5 GalA residues,<sup>236</sup> while petunia-solubilized GalAT activity added up to 27 GalA residues,<sup>235</sup> with the number of residues added being dependent on the concentration of UDP-GalA used. The bulk of the *in vitro* HG:GalAT data from multiple sources strongly suggests that the characterized HG:GalATs are not processive.

The first gene encoding an HG:GalAT was isolated from Arabidopsis suspension culture cells.<sup>228</sup> LC-MS/MS of trypsin-digested partially purified solubilized Arabidopsis GalAT active fractions identified two proteins in a NCBI BLAST (<http://www.ncbi.nlm.nih.gov/>) of protein sequences corresponding to GAUT1 (At1g61130) and GAUT7 (At2g38650), members of the galacturonosyltransferase1(GAUT1)-related gene family. Anti-GAUT1 polyclonal antibodies were able to immunoadsorb GalAT activity from the partially purified Arabidopsis solubilized GalAT enzyme preparations, providing evidence that the GAUT1 gene encodes a pectin biosynthetic HG:GalAT.<sup>228</sup>

The open reading frames of GAUT1 and GAUT7 were amplified from Arabidopsis RNA and truncated to remove the trans-

membrane domain for expression in human embryonic kidney (HEK293) cells. A *Trypanosoma cruzi* mannosidase signal sequence and C-terminal HA epitope tag were engineered onto GAUT1 and GAUT7 allowing the recombinant protein to be secreted directly to the culture medium. The truncated GAUT1 and GAUT7 proteins were recovered from the HEK cell medium by immunoprecipitation with anti-HA antibodies from the cell medium. GAUT1, but not GAUT7, immunoprecipitates yielded incorporation of [<sup>14</sup>C]GalA into discretely sized OGA acceptors when incubated with UDP-[<sup>14</sup>C]GalA. GAUT1 catalyzed elongation of OGA acceptors in an  $\alpha$ -(1,4)-configuration; an activity consistent with a role of GAUT1 as an HG:GalAT in pectin biosynthesis.

The GAUT1 and GAUT7 amino acid sequences are part of a distinct subfamily, which includes 15 GAUT genes and 10 GATL genes, of the CAZy database (<http://www.cazy.org/>)<sup>240</sup> GT8 family. The GAUT1-related family is defined by a C-terminal amino acid motif common to both the GAUT and GATL proteins, but that is not a characteristic of other GT8 member proteins: [H-[FWY]-[DNS]-G-x(2)-K-P-W-x(2)-[ILH]-[ADGS]].<sup>228</sup> The GAUT and GATL proteins are each defined by additional amino acid motifs unique to each group (Fig. 12). It has been proposed that the GAUT1-related gene family encodes GalATs required to synthesize the many specific GalpA linkages of the wall complex polysaccharides (see Table 4). Further study of this gene family may lead to the discovery of many unique GalAT activities. In addition, many new structures may be identified in the process of defining the expression patterns

**Table 3**  
Predicted and proven *A. thaliana* nucleotide-sugar interconverting enzymes required for pectin biosynthesis<sup>a</sup>

Enzyme	NDP-sugar <sup>b</sup>	Enzymatic reaction <sup>c</sup>	Isoform	Locus <sup>d</sup>	Reference
UDP-glucose epimerase (UGE)	UDP-Glc	E.C.5.1.3.2	UGE1	At1g12780	199,200
			UGE2	At4g23920	200
			UGE3	At1g63180	200
			UGE4/RHD1	At1g64440	201–203,200
			UGE5	At4g10960	200
UDP-xylose epimerase (UXE)	UDP-Ara	E.C.5.1.3.5	UXE1/MUR4	At1g30620	204,205
			UXE2	At4g20460	
			UXE3	At2g34850	
			UXE4	At5g44480	
UDP-glucuronic acid epimerase (GAE)	UDP-GalA	E.C.5.1.3.6	GAE1/UGlcAe3	At4g30440	206
			GAE2/UGlcAe5	At1g02000	206
			GAE3/UGlcAe4	At4g00110	206
			GAE4/UGlcAe1	At2g54310	
			GAE5/UGlcAe6	At4g12250	
			GAE6/UGlcAe2	At3g23820	
UDP-glucose dehydrogenase (UGD)	UDP-Gal	E.C.1.1.1.22	UGD1	At5g39320	207,208
			UGD2	At3g29360	208
			UGD3	At5g15490	208
			UGD4	At1g26590	208
UDP-xylose synthase (UXS)	UDP-Xyl	E.C.4.1.1.35	UXS1/AUD3	At3g53520	209
			UXS2/AUD1	At3g62830	209
			UXS3/SUD2	At5g59290	209
			UXS4/AUD2	At2g47650	
			UXS5/SUD1	At3g46440	
UDP-rhamnose synthase (RHM)	UDP-l-Rha	E.C.4.2.1.76 <sup>d</sup>	RHM1/URS1	At1g78570	210,51,211
			RHM2/MUM4	At1g53500	
			RHM3	At3g14790	
			UER1	At1g63000	
UDP-apiiose/UDP-xylose synthase (AXS)	UDP-Api/UDP-Xyl	e	AXS1	At2g27860	212
			AXS2	At1g08200	
GDP-mannose dehydrogenase (GMD)	GDP-4-keto-6-deoxy-Man	E.C.4.2.1.47	GMD1	At5g66280	213,214
			GMD2/MUR1	At3g51160	136,215,213,214,216
GDP-mannose epimerase/reductase (GER)	GDP-Fuc	e	GER1	At1g73250	217,216
			GER2	At1g17890	
GDP-mannose epimerase (GME)	GDP-l-Gal	E.C.5.1.3.18	GME1	At5g28840	218–220
Kdo synthase (KDS)	CMP-Kdo	E.C.2.5.1.55	KDSA1/KdopS <sup>g</sup>	At1g79500	221,222
			KDSA2	At1g16340	221
CMP-Kdo synthase (CKS)	CMP-Kdo	E.C.2.7.7.38			f
<i>myo</i> -inositol oxygenase (MIOX)	D-GlcA	E.C.1.13.99.1	MIOX4	At4g26260	223
				At5g56640	223
				At2g19800	223
				At1g14520	223

<sup>a</sup> Adapted from Seifert et al. (2004).<sup>b</sup> The nucleotide-sugar synthesized.<sup>c</sup> The Enzyme Commission number (E.C.x.x.x.x) of each enzyme activity is listed based on the chemical reaction carried out.<sup>d</sup> The locus of the Arabidopsis gene is given as the AGI code that refers to the position of the gene on Arabidopsis chromosomes.<sup>e</sup> The RHM has catalytic activities equivalent to the combined bacterial E.C. 5.1.3.13, E.C. 1.1.1.133 and E.C. 4.2.1.76.<sup>f</sup> E.C. numbers were not assigned for these activities.<sup>g</sup> CMP-Kdo synthase enzymes have not been identified in Arabidopsis; however, the protein and corresponding gene have been identified in maize (*ZmCKS*) and a putative protein accession number has been identified in Arabidopsis (AC007202).

and the specific linkages catalyzed by the genes of the GAUT1-related gene family.

A subfraction of HG is composed of XGA; HG decorated with xylose residues at the O-3 of backbone GalA residues.<sup>29</sup> A xylosyltransferase in Arabidopsis was identified that is reported to be an XGA xylosyltransferase.<sup>241</sup> This would be the first glycosyltransferase identified in the synthesis specifically of XGA.

#### 5.4. Pectin methyltransferase

The modification of pectic polysaccharides by addition of methyl groups at the C-6 carboxyl group, or acetyl groups at the O-2 or O-3 of GalA residues is regulated in a developmental manner.<sup>242</sup> Pectin methyltransferases (PMTs) act specifically on pectic

polysaccharides during synthesis in the Golgi apparatus. Pectins are secreted in a highly methylesterified form.<sup>243,244</sup> After the deposition of pectins in the apoplast, pectic methylesterases (PMEs) selectively remove the methyl groups. The extent and pattern of methylation of pectic polysaccharides affect the functional characteristics of the pectic polysaccharides,<sup>245</sup> for example, by altering the affinity of pectins for calcium ions and altering the accessibility of pectins to wall hydrolases.<sup>16</sup> The pectic polysaccharides are methylated by PMTs that catalyze the transfer of a methyl group from the donor *S*-adenosyl-methionine (SAM) to the target pectic polysaccharide.<sup>229,246,247</sup> The import of SAM into the Golgi lumen is necessary for the methylation of HG<sup>248</sup> where PMT activities have been localized.<sup>249–251</sup> The catalytic activity of PMTs has been detected and partially characterized in the extracts of

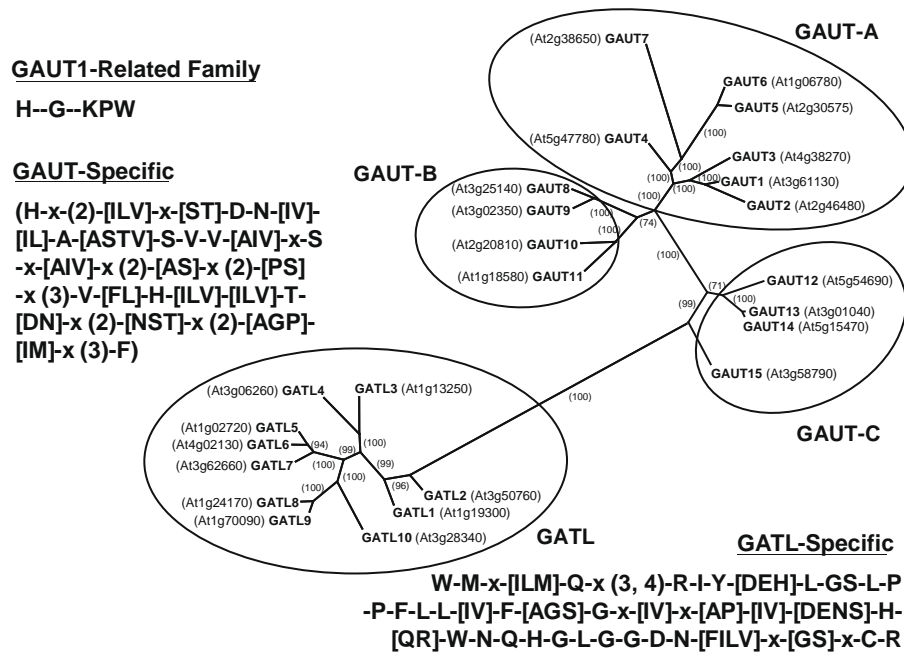


**Figure 12.** The Arabidopsis GAUT1-related gene family as defined by Sterling et al. (2006). The *A. thaliana* galacturonosyltransferase-1 (GAUT)-related gene family has 15 GAUT genes and 10 GAUT-like (GATL) genes. Proteins in the GAUT1-related gene family have shared amino acid motifs not conserved among other GT8 proteins. The GAUT and GATL proteins also have unique defining amino acid motifs.

**Table 4**  
Pectin biosynthetic galacturonosyltransferase (GalAT) activity

Plant source	Fraction <sup>a</sup>	pH optimum	Apparent $K_m$ for UDP-GalpA ( $\mu\text{M}$ )	$V_{\max}$ ( $\text{pmol min}^{-1} \text{mg}^{-1}$ )	Acceptor <sup>b</sup>	Reference
<i>Vigna radiata</i>	Particulate	6.3–7.0	1.7	4700	Endogenous	229
<i>Vigna radiata</i>	Particulate	ND	ND	ND	Endogenous	230
<i>Brassica rapa</i>	Particulate	ND	ND	ND	Endogenous	230
<i>Lycopersicon esculentum</i>	Particulate	ND	ND	ND	Endogenous	230
<i>Acer pseudoplatanus</i>	Particulate	ND	770	ND	Endogenous	231
<i>Nicotiana tabacum</i>	Particulate	7.8	8.9	150	Endogenous	232,233
<i>Nicotiana tabacum</i>	Solubilized	6.3–7.8	37	290	Exogenous/endogenous	21,162
<i>Vigna angularis</i>	Permeabilized	6.8–7.8	140	1650	Exogenous	234
<i>Pisum sativum</i>	Permeabilized	ND	ND	ND	Exogenous/endogenous	177
<i>Petunia axillaris</i>	Solubilized	7.0	170	640	Exogenous	235
<i>Cucurbita moschata</i>	Particulate	6.8–7.3	1700	15,000	Exogenous	236
<i>Arabidopsis thaliana</i>	Solubilized	ND	ND	ND	Exogenous	228
<i>Pisum sativum</i>	Particulate	ND	ND	ND	Exogenous	237

ND: Not determined.

<sup>a</sup> The activity was detected from membrane particulate preparations (particulate), detergent-permeabilized membranes (permeabilized) or detergent-solubilized membranes (solubilized).

<sup>b</sup> The acceptor may be endogenous (that existing in the preparation) or exogenous (previously extracted pectins of variable purity).

multiple plant species (Table 5): mung bean (*V. radiata*),<sup>252</sup> flax (*Linus usitatissimum*),<sup>253</sup> tobacco (*N. tabacum*),<sup>254</sup> and soy bean (*G. max*).<sup>255</sup>

Multiple PMT enzymes are required for pectin synthesis as evidenced by the discovery of PMT isoforms in flax Golgi membranes separated in sucrose density gradients. The PMT isoforms were identified as PMT activities that had distinct pH optima and also had a differential preference for substrates with high or low levels of pectin methylation.<sup>256</sup> Indeed, an assortment of PMTs may be required to form the methylesters of HG in a regulated fashion.

The biosynthesis of pectin is dependant on the action of PMTs. It was shown in flax<sup>256</sup> and mung bean<sup>257</sup> that addition of exogenous pectin acceptors increased rates of PMT activity. Excessive SAM substrate, however, does not have this effect on PMT activity. Flax microsomal membranes yielded three partially purified polypeptides of distinct sizes with PMT activity: PMT5 (40 kDa), PMT7 (110 kDa), and PMT18 (18 kDa). The PMT18 protein appeared to harbor PMT activity and was found in partially purified prepara-

tions of both PMT5 and PMT7, suggesting that PMT18 may be the catalytic subunit of PMT5 and PMT7. Confirmation that these proteins are PMTs has not yet been presented. Mutagenesis of the Arabidopsis genome has led to the identification of a putative PMT mutant at the At1g78240 gene locus that is predicted to encode a ~43 kDa protein with sequence similarity to known methyltransferases. The mutant is referred to as the *quasimodo-2/tumorous shoot development-2* (*qua2/tsd2*) mutant.<sup>249,258</sup> Based on the conservation of the MT domain of QUA2/TSD2, the Arabidopsis genome contains 29 putative PMT homologs, while rice has at least 14 conserved homologs. The catalytic activity of QUA2/TSD2 has not been definitively determined, either in vivo or in vitro. Evidence for QUA2/TSD2 PMT function in pectin biosynthesis is its pleiotropic phenotype similar in several respects to *qua1*, a putative pectin HG:GalAT.<sup>261</sup> *Qua2/tsd2* has reduced cell adhesion, particularly at the meristems, and is specifically reduced in HG, but not RG-I pectic polysaccharides.<sup>249,258</sup> Interestingly, the QUA2 transcript was found to be co-expressed with *QUA1/GAUT8*, sug-



**Table 5**  
Pectin biosynthetic pectin methyltransferase (PMT) activity

Plant source	Fraction <sup>a</sup>	pH optimum	Apparent $K_m$ for SAM ( $\mu\text{M}$ )	$V_{\text{max}}$ ( $\text{pmol min}^{-1} \text{mg}^{-1}$ )	Acceptor <sup>b</sup>	Reference
<i>Vigna radiata</i>	Particulate	6.8	59	2.7	HG	252,247,257
<i>Linus usitatissimum</i>	Particulate	6.8	10–30	ND	HG	253
<i>Linus usitatissimum</i>	Solubilized	7.1	30	ND	HG	246
<i>Linus usitatissimum</i>	Particulate	5.5	20	ND	Low MeOxy-HG	256,256,259
<i>Linus usitatissimum</i>	Particulate	7.0	20	ND	High MeOxy-HG	256,256,259
<i>Nicotiana tabacum</i>	Particulate	7.8	38	49	HG	254,250
<i>Nicotiana tabacum</i>	Solubilized	7.8	18	7.3	HG	260
<i>Glycine max</i>	Permeabilized	6.8	230	600–1300	HG	255
<i>Linus usitatissimum</i>	Solubilized <sup>c</sup>	ND	ND	ND	HG	259

ND: Not determined.

<sup>a</sup> Particulate (particulate), detergent-permeabilized (permeabilized) or detergent-solubilized (solubilized) membranes were used.

<sup>b</sup> The HG acceptor, with variable levels of further characterization except where noted (high or low Methyl-esterified HG (MeOxy-HG)).

<sup>c</sup> The PMT activity was further purified from a solubilized membrane preparation to yield PMT5, PMT7, and PMT18.

gesting a functional linkage between QUA1 and QUA2. The transcripts of additional QUA2 isoforms were co-expressed with GAUT9 and GAUT1.<sup>249</sup> The cooperativity of PMT activity with exogenously added HG acceptors in mung bean<sup>247</sup> and the co-expression of GAUT and PMT transcripts, may reflect a physical dependence of HG:GalATs on PMTs.

### 5.5. Pectin acetyltransferase

Pectin *O*-acetyltransferase (PAT) activity catalyzes the transfer of an acetyl group from acetylCoA to a pectic polysaccharide acceptor. Acetyl groups decorate the GalA residues of pectic polysaccharides at the O-2 or O-3 positions.<sup>262</sup> Acetyl groups may decorate the GalpA residues of HG and RG-I; however, acetylation was not detected on the RG-II backbone.<sup>262</sup> *O*-acetylation was detected, however, on the 4-*O*-methyl-fucose residue and aceric acid residue of RG-II sidechain B.<sup>263</sup> The functional consequences of acetylation are not clear but may play a role in preventing pectin breakdown by microbial hydrolases. PAT activity has been detected in microsomal membrane preparations of potato.<sup>264</sup> The PAT activity at 30 °C was found to have a pH optimum of 7.0, an apparent  $K_m$  of 35  $\mu\text{M}$  for acetyl-CoA and a  $V_{\text{max}}$  of 0.9  $\text{pkat mg}^{-1} \text{protein}$ .<sup>264</sup>

### 5.6. RG-I glycosyltransferases

The biosynthesis of RG-I requires multiple glycosyltransferase activities to synthesize a backbone of [ $\rightarrow 2$ ]- $\alpha$ -L-Rhap-(1,4)- $\alpha$ -D-GalpA-(1 $\rightarrow$ ) disaccharide repeats that are branched at the C-4 of approximately half of the rhamnose residues by 5-linked and 3,5-linked arabinan, 4-linked and 4,6-linked galactan, as well as Type-I and Type-II AG.<sup>1</sup> Potentially 34 specific activities may be required to synthesize RG-I backbone (see Table 2).<sup>164,265</sup>

The  $\alpha$ 1,4-rhamnosyltransferase ( $\alpha$ 1,4-RhaT) and  $\alpha$ -1,2-galacturonosyltransferase ( $\alpha$ 1,2-GalAT) responsible for synthesis of the RG-I backbone have not been identified. Bacterial genes are useful as potential models with which to query plant genomes and may be of use in identification of the RG-I:RhaT. Recently, an  $\alpha$ 1,3-RhaT (WapR) and an  $\alpha$ 1,6-RhaT (MigA) were identified in *Pseudomonas aruginosa* that are responsible for the transfer of rhamnosyl residues to the core glycan structure of lipopolysaccharide (LPS).<sup>266</sup> Bacterial nucleotide interconverting genes have successfully been used to identify the nucleotide interconverting enzymes UGE1 in *Arabidopsis* from *Streptococcus pneumoniae* Cap1J bacterial UGE.<sup>206,267</sup> The RHM2 in *Arabidopsis* was identified from bacterial protein family hidden markov models (HMM) of NDP-rhamnose synthesis (PFAM; PF01370).<sup>210</sup> In addition, hydrophobic cluster analysis in conjunction with the identified conserved glycosyltransferase domains of *Acetobacter xylinium* cellulose synthase (CesA) was used to identify CesA homologs in plants.<sup>66,268</sup> Hydrophobic cluster analysis aids in the identification of homologs across

species that may not retain great conservation of the primary amino acid sequence but retain function based on the secondary protein structure predicted by hydrophobic amino acid clustering.<sup>269</sup> These methods provide hope for identification of additional pectin GTs in the future.

### 5.7. RG-I galactosyltransferases

The galactan side chains of RG-I are composed primarily of  $\beta$ -1,4-D-galactan with some branches of  $\beta$ -1,6- and  $\beta$ -1,3-Gal. The galactosyltransferases (GalTs) catalyze transfer of D-Galp residues from UDP-D-Galp to an acceptor molecule. Pectin GalTs are hypothesized to catalyze the initiation of galactan side chains directly onto the backbone Rhap residues of RG-I, elongate galactan chains, initiate branch points onto galactan chains, and elongate galactan side chains. Synthesis of these structures may require up to 10 or more different pectin-specific GalTs (see Table 2).<sup>164,265</sup>

The characterization of GalT activities necessary for RG-I galactan biosynthesis has been carried out in flax,<sup>270</sup> mung bean,<sup>271</sup> potato,<sup>272</sup> radish,<sup>273</sup> and soybean<sup>274</sup> (Table 6). The  $\beta$ 1,4-GalT activity of potato,<sup>178</sup> radish,<sup>273</sup> and pea homogenates<sup>275</sup> was localized to the Golgi apparatus by sucrose density gradient centrifugation. Fractionation of Golgi membranes into high-, medium-, and low-density microsomes showed that the galactan  $\beta$ 1,4-GalT activity had a differential distribution in density gradients from glycoprotein GalT activity.<sup>276</sup> The products of the above pectin GalT activity were not characterized, and thus, may represent both elongating and branching galactan GalT activities.

Pectin RG-I:GalT activity that specifically elongates existing Gal branches on the RG-I backbone was recovered from microsomal membrane preparations of mung bean. The GalTs catalyzed the transfer of a Galp onto  $\beta$ -1,4-galactan acceptor molecules.<sup>271,277</sup> Cleavage of the reaction products specifically by endo- $\beta$ -1,4-galactanase verified the linkage catalyzed. Similar experiments were carried out in potato<sup>272</sup> and soybean.<sup>274</sup> The GalT activity in pea microsomal membranes elongated a  $\beta$ -1,4-galactan acceptor that was associated with a high molecular weight PG- and RG-A lyase-digestible pectin.<sup>280</sup> The partially purified pectin biosynthetic GalT activity isolated from soybean was able to transfer more than 25 galactosyl units onto an oligogalactan of DP 7, which is approaching the length of native pectin galactan branches isolated from soybean RG-I.<sup>281</sup> The GalT activity that elongates a growing galactan chain is discerned from GalT activity that initiates a Gal linkage onto the rhamnosyl C-4 of the RG-I backbone or onto the C-4 of an existing Gal linked to the RG-I backbone. GalT activity that utilizes a [ $\beta$ -D-Galp-(1 $\rightarrow$ 4)- $\alpha$ -L-Rhap-(1 $\rightarrow$ )] acceptor was identified in potato microsomal membranes.<sup>279</sup> This GalT activity was suggestive of a chain initiation GalT that adds a single Gal onto the firstly added Gal on the RG-I backbone. Such an activity would catalyze the second initiating step in RG-I galactan

**Table 6**  
Pectin biosynthetic galactosyltransferase (GalT) activity

Plant source	Fraction <sup>a</sup>	pH optimum	Apparent $K_m$ for UDP-Galp ( $\mu\text{M}$ )	$V_{max}$ ( $\text{pmol min}^{-1} \text{mg}^{-1}$ )	Linkage	Acceptor <sup>b</sup>	Reference
<i>Linum usitatissimum</i>		8.0	38	75	$\beta$ -1,4-	Endogenous	270
<i>Linum usitatissimum</i>		5.0	38	75	$\beta$ -1,3 or $\beta$ -1,6-	Endogenous	270
<i>Vigna radiata</i>		6.5	ND	ND	$\beta$ -1,4-	Endogenous	271
<i>Solanum tuberosum</i>	Particulate	6.0	ND	ND	$\beta$ -1,4-	Endogenous RG-I/exogenous galactan	272,178
<i>Linum usitatissimum</i>	Solubilized	8.0	460	180	$\beta$ -1,4-	Exogenous RG-I/galactan	278
<i>Solanum tuberosum</i>	Solubilized	7.5	ND	ND	$\beta$ -1,4-	Exogenous RG-I/galactan	279
<i>Solanum tuberosum</i>	Solubilized	5.6	ND	ND	?	Exogenous RG-I/galactan	279
<i>Pisum sativum</i>	Particulate	7.0–8.0	ND	ND	$\beta$ -1,4-	Endogenous RG-I/galactan/XG	280
<i>Raphanus sativus</i>	Particulate	5.9–6.3	410	1000	$\beta$ -1,6-	Exogenous RG-I/galactan	273
<i>Vigna radiata</i>	Permeabilized	6.5	32	200	$\beta$ -1,4-	Exogenous $\beta$ -1,4-galactan	277
<i>Glycine max</i>	Permeabilized	6.5	1200	2000–3000	$\beta$ -1,4-	Exogenous $\beta$ -1,4-galactan	274
<i>Glycine max</i>	Solubilized	6.5	ND	17,000	$\beta$ -1,4-	Exogenous $\beta$ -1,4-galactan	274,281

ND: Not detected, ?: unknown linkage.

<sup>a</sup> Particulate (particulate), detergent-permeabilized (permeabilized) or detergent-solubilized (solubilized) membranes were used.

<sup>b</sup> The acceptor molecules used in the references listed were both endogenous and exogenous and have been characterized to a greater or lesser degree; additional information is noted as available.

synthesis. This activity catalyzed the addition of Gal residues from UDP-[<sup>14</sup>C]galactose onto small RG-I backbone fragments with a low degree of galactosylation, but not onto RG-I with a high degree of galactosylation, RG-I without galactosylation, galactan, or galactooligomers. In addition, the activity was separable from a different  $\beta$ 1,4-GalT activity that did incorporate [<sup>14</sup>C]Gal onto highly galactosylated RG-I.<sup>279</sup> Similarly, a GalT activity isolated from flax elongated existing single Gal residues of RG-I; a potential GalT involved in galactan chain initiation.<sup>278</sup>

The  $\beta$ -1,3-galactan and  $\beta$ -1,6-galactan structures are primarily associated with wall AGPs; however, some have been isolated in association with RG-I sidechains. A GalT activity isolated from 6-day old radish root microsomal membrane preparations showed elongation of  $\beta$ -1,3- and  $\beta$ -1,6-galactooligomers.<sup>273</sup> The elongation of de-arabinosylated AGs from AGP polysaccharides was also elongated by the GalT in these fractions.<sup>273</sup>

The Arabidopsis *MUR3* encodes a glycosyltransferase in GT47 that is predicted to be an XG-GalT. GT47 has 9 subfamilies (A, B, C1, C2, C3, D1, D2, E, and F) that show varying similarity to animal exostosins. *MUR3* is a putative GalT based on wall glycosyl residue composition phenotype that has a distinct reduction in wall Gal content. Further characterization of the *mur3* mutant plants that had a wild-type-like phenotype revealed via wall analyses that the xyloglucan of *mur3* mutant plants had reduced galactosylation. The enzymatic activity of heterologously expressed *MUR3* showed activity of a galactosyltransferase that is specific for transfer of a galactose to the third xylose substituted Glc in a xyloglucan XXXG unit.<sup>282</sup> Whether any of the other GT47 family members are GalTs involved in RG-I synthesis, remains to be determined.

### 5.8. RG-I arabinosyltransferase

The synthesis of  $\alpha$ -1,5-linked arabinan by  $\alpha$ 1,5-AraT involves the transfer of Ara residues from UDP-L-Araf to acceptor molecules

in an  $\alpha$ -(1,5) configuration. As many as 18 AraTs may be required for the synthesis of the complex branched arabinans of pectic polysaccharides.<sup>265</sup> AraT activity has been characterized in mung bean<sup>179</sup> and French bean<sup>283</sup> (Table 7). Pectin biosynthetic AraT activity is derived from membrane fractions and requires  $\text{Mn}^{2+}$  ions.

Arabinan AraT activity was first observed in mung bean permeabilized microsomal membranes.<sup>284</sup> The product of addition of [<sup>14</sup>C]arabinose to mung bean permeabilized membranes was an arabinan, as characterized by paper chromatography of the sugars released by acid hydrolysis.<sup>284</sup> Similar experiments carried out in French bean produced products that were degraded by pectinase;<sup>283</sup> however, structural characterization of the acceptor was not carried out. In 1992, a partially purified 70 kDa putative AraT was recovered from active protein fractions using a monoclonal antibody found to inhibit AraT activity in microsomal membranes.<sup>285</sup> Despite the repeated solubilization of AraT activity and the partial purification of a putative AraT protein, the AraT was not identified and the enzyme products of the putative AraT were not rigorously characterized. Recently, however, an authentic  $\alpha$ 1,5-AraT activity was observed by the incubation of UDP-L-Araf with mung bean hypocotyl Golgi membranes and exogenous  $\alpha$ -1,5-L-arabinooligosaccharides. The products were determined to be  $\alpha$ -1,5-linked by  $\alpha$ -L-arabinofuranosidase cleavage and NMR structure determination.<sup>288</sup>

The complex branched arabinans of pectic RG-I polysaccharides also require the activities of a  $\beta$ 1,3-AraT that was identified in mung bean membrane preparations.<sup>179,186,287</sup> The mung bean Golgi-enriched membranes incorporated L-[<sup>14</sup>C]Araf onto endogenous 1,5-linked arabinofuranooligos, but very inefficiently. The reaction products were not released with an  $\alpha$ 1,5-arabinofuranosidase and only approximately 25% of the radio-labeled products were released by an arabinofuranosidase that cleaved 1,2-, 1,3-, or 1,5-linkages.<sup>179</sup> Similar activity assays were carried out with mung

**Table 7**  
Pectin biosynthetic arabinosyltransferases (AraT) activity

Plant source	Fraction <sup>a</sup>	pH optimum	Apparent $K_m$ for UDP-Ara ( $\mu\text{M}$ )	$V_{max}$ ( $\text{pmol min}^{-1} \text{mg}^{-1}$ )	Linkage	Acceptor <sup>b</sup>	Reference
<i>Vigna radiata</i>	Permeabilized	6.0–6.5	ND	ND	? Ara	Endogenous	284
<i>Phaseolus vulgaris</i>	Particulate	ND	178	ND	? AraT	Endogenous	286,283
<i>Phaseolus vulgaris</i>	Solubilized	ND	ND	199,000	?-Ara	Endogenous	285
<i>Vigna radiata</i>	Solubilized	6.5	33,000	ND	?-AraT	Exogenous $\alpha$ -1,5-arabinan	179
<i>Vigna radiata</i>	Solubilized	6.5–7.0	550	1700	$\beta$ -1,3-Araf	Exogenous $\alpha$ -1,5-arabinan	287
<i>Vigna radiata</i>	Solubilized	6.0–6.5	330	200	$\beta$ -1,4-Araf	Exogenous $\beta$ -1,4-galactan	186
<i>Vigna radiata</i>	Solubilized	6.5–7.0	234	ND	$\alpha$ -1,5-Araf	Exogenous $\alpha$ -1,5-arabinan	288

ND: Not detected, ?: unknown linkage.

<sup>a</sup> Particulate (particulate), detergent-permeabilized (permeabilized) or detergent-solubilized (solubilized) membranes were used.

<sup>b</sup> The acceptors utilized in the referenced studies were endogenous or exogenous with variable degrees of characterization; added information is listed where available.

bean Golgi membranes incubated with UDP- $\beta$ -L-Arap and 2-amino-benzamide (2-AB) labeled 1,5-linked arabinofuranoheptasaccharides. The reaction products were found to be  $\beta$ -1,3-Arap residues linked to the terminal AraF residues of the 2-AB labeled acceptors.<sup>186</sup> The linkage and ring conformation of the terminal  $\beta$ -linked residue were confirmed by partially methylated alditol acetates and NMR spectroscopy.<sup>186</sup>

A  $\beta$ 1,4-ArapT activity was identified which catalyzes the transfer of a terminal  $\beta$ -Arap from UDP- $\beta$ -L-Arap onto the terminal non-reducing residue of a  $\beta$ -1,4-galactooligosaccharide labeled at the reducing end with 2-AB.<sup>287</sup> The conformation of the reaction products was determined by ESI-MS/MS, linkage analysis, and NMR. The linkage described naturally occurs in RG-I galactan side-chains.<sup>56</sup> The Ara1Gal7-2-AB molecule was not further utilized as an acceptor for either AraT or GalT activity, suggesting that the terminal Ara residue may act as a cap or terminator of RG-I sidechain synthesis.<sup>287</sup>

The Arabidopsis T-DNA insertion mutant *arad1* has reduced cell wall arabinan with little change in the composition of other glycosyl residues and no apparent physical phenotype and is hypothesized to be a putative cell wall AraT.<sup>289</sup> The mutant wall compositional phenotype was complemented by the ARAD1 transgene under the 35S promoter. ARAD1 (At2g35100) is a GT47 glycosyltransferase that has 7 additional Arabidopsis homologs and 4 rice homologs.<sup>289</sup>

### 5.9. RG-II glycosyltransferase

The backbone on RG-II is  $\alpha$ -1,4-D-GalA-linked HG. GAUT1 has recently been discovered, which catalyzes the addition of GalA residues onto HG oligomers,<sup>228</sup> and could, conceivably, synthesize the backbone of RG-II. There are 15 GAUT genes in the GAUT1-related gene family, and it is also possible that one of these may function to specifically synthesize the backbone of RG-II. Further work in this area will be needed to explore this possibility, because the acceptor specificities for the GAUTs have not been determined.

A putative glucuronosyltransferase (GlcAT) was identified in a screen for intercellular adhesion defects in T-DNA transformants of *nolac-H18/irx10*. The gene identified that causes the *nolac* phenotype had nucleotide sequence similarity to the human, *Caenorhabditis elegans*, and *Drosophila melanogaster* heparin sulfate GlcAT exostosin 2 (EXT2).<sup>138</sup> Complementation of the mutant with *NpGUT1* under the 35S promoter returned WT-like cellular adhesion to the cells. Because the mutant was shown to have reduced efficiency for RG-II borate dimer formation and reduced GlcA in purified RG-II preparations, the linkage disrupted was hypothesized to be the RG-II sidechain A GlcA residue that is linked to the C-4 of the Fuc residue. The absence of this residue would also eliminate a Gal residue linked to the C-2 of the GlcA residue. The activity of the protein encoded by GUT1/IRX10 has not been determined and some evidence suggests a role in secondary cell wall biosynthesis.<sup>290</sup> Currently, other GTs that act to synthesize RG-II sidechain structures are not known, leaving large informational gaps in the biosynthesis of RG-II.

## 6. Conclusions and relevance

The research on pectin structure, techniques for pectin analysis, pectin function in plant growth, and pectin biosynthesis is rapidly advancing in the genomic age. Genes may be identified by sequence similarity to those in databases and targeted for cloning or mutagenesis. Clearly, today the tools are available to tackle the existing gaps in the knowledge of pectin structure, function, and biosynthesis.

Areas of pectin research which are lagging include the identification of GTs responsible for the biosynthesis of pectin. Progress has been made in recent years, however, GT activities for less than a handful of linkages have been characterized and fewer genes have been identified. Generally speaking, the substrates and acceptors must frequently be generated by each researcher in order to carry out the analyses. Undoubtedly, the lack of discoveries in pectin biosynthesis is in-part due to the difficulty with which the activities may be assayed.

### Acknowledgments

This project was supported in part by NSF MCB awards 0313509 and 0646109, NRI, CSREES, USDA Awards 2003-35318-15377 and 2006-35318-17301 and DOE DE-FG02-93-ER20097. The BioEnergy Science Center is a collaborative effort between Oak Ridge National Laboratory and other research sites, for more information please go to [www.bioenergycenter.org](http://www.bioenergycenter.org).

### References

- Ridley, B. L.; O'Neill, M. A.; Mohnen, D. *Phytochemistry* **2001**, *57*, 929–967.
- O'Neill, M. A.; York, W. S. *An. Plant Rev.* **2003**, *8*, 1–35.
- Carpita, N. C. *Annu. Rev. Plant Physiol. Plant Mol. Biol.* **1996**, *47*, 445–476.
- Selvendran, R. R.; O'Neill, M. A. *Methods Biochem. Anal.* **1987**, *32*, 25–153.
- Bush, M. S.; Marry, M.; Huxham, I. M.; Jarvis, M. C.; McCann, M. *Planta* **2001**, *213*, 869–880.
- Zablackis, E.; Huang, J.; Muller, B.; Darvill, A. G.; Albersheim, P. *Plant Physiol.* **1995**, *107*, 1129–1138.
- Talmadge, K. W.; Keegstra, K.; Bauer, W. D.; Albersheim, P. *Plant Physiol.* **1973**, *51*, 158–173.
- Seymour, G. B.; Colquhoun, I. J.; DuPont, M. S.; Parsley, K. R.; Selvendran, R. R. *Phytochemistry* **1990**, *29*, 725–731.
- Muda, P.; Seymour, G. B.; Errington, N.; Tucker, G. A. *Carbohydr. Polym.* **1995**, *26*, 255–260.
- Willats, W. G. T.; McCartney, L.; Knox, J. P. *Planta* **2001**, *213*, 37–44.
- Mort, A. J.; Qiu, F.; Maness, N. O. *Carbohydr. Res.* **1993**, *247*, 21–35.
- Liners, F.; Letesson, J.-J.; Didembourg, C.; Van Cutsem, P. *Plant Physiol.* **1989**, *91*, 1419–1424.
- Jarvis, M. C.; Apperley, D. C. *Carbohydr. Res.* **1995**, *275*, 131–145.
- Yoo, S.-H.; Fishman, M. L.; Savary, B. J.; Hotchkiss, A. T. *J. Agric. Food Chem.* **2003**, *51*, 7410–7417.
- Popper, Z. A.; Fry, S. *Planta* **2007**, *227*, 781–794.
- Benen, J. A. E.; Kester, H. C. M.; Visser, J. *Eur. J. Biochem.* **1999**, *259*, 577–585.
- York, W. S.; Kolli, V. S. K.; Orlando, R.; Albersheim, P.; Darvill, A. G. *Carbohydr. Res.* **1996**, *285*, 99–128.
- Keegstra, K.; Talmadge, K. W.; Bauer, W. D.; Albersheim, P. *Plant Physiol.* **1973**, *51*, 188–196.
- Nakamura, A.; Furuta, H.; Maeda, H.; Takao, T.; Nagamatsu, Y. *Biosci., Biotechnol., Biochem.* **2002**, *66*, 1301–1313.
- Popper, Z. A.; Fry, S. C. *Ann. Bot.* **2005**, *96*, 91–99.
- Doong, R. L.; Mohnen, D. *Plant J.* **1998**, *13*, 363–374.
- Thibault, J.-F.; Renard, C. M. G. C.; Axelos, M. A. V.; Roger, P.; Crepeau, M.-J. *Carbohydr. Res.* **1993**, *238*, 271–286.
- Yapo, B. M.; Lerouge, P.; Thibault, J.-F.; Ralet, M.-C. *Carbohydr. Polym.* **2007**, *69*, 426–435.
- Hart, D. A.; Kindel, P. K. *Biochem. J.* **1970**, *116*, 569–579.
- Ovodov, Y. S.; Ovodova, R. G.; Bondarenko, O. D.; Krasikova, I. N. *Carbohydr. Res.* **1971**, *18*, 311–318.
- Longland, J. M.; Fry, S. C.; Trewas, A. J. *Plant Physiol.* **1989**, *90*, 972–976.
- Schols, H. A.; Posthumus, M. A.; Voragen, A. G. J. *Carbohydr. Res.* **1990**, *206*, 117–129.
- Nakamura, A.; Furuta, H.; Maeda, H.; Takao, T.; Nagamatsu, Y. *Biosci., Biotechnol., Biochem.* **2002**, *66*, 1155–1158.
- Le Goff, A.; Renard, C. M. G. C.; Bonnin, E.; Thibault, J.-F. *Carbohydr. Polym.* **2001**, *45*, 325–334.
- Schols, H. A.; Vierhuis, E.; Bakx, E. J.; Voragen, A. G. J. *Carbohydr. Res.* **1995**, *275*, 343–360.
- Zandleven, J.; Sorensen, S. O.; Harholt, J.; Beldman, G.; Schols, H. A.; Scheller, H. V.; Voragen, A. J. *Phytochemistry* **2007**, *68*, 1219–1226.
- Darvill, A.; McNeil, M.; Albersheim, P. *Plant Physiol.* **1987**, *62*, 418–422.
- Spellman, M. W.; McNeil, M.; Darvill, A. G.; Albersheim, P. *Carbohydr. Res.* **1983**, *122*, 115–129.
- Stevenson, T. T.; Darvill, A. G.; Albersheim, P. *Carbohydr. Res.* **1988**, *179*, 269–288.
- York, W. S.; Darvill, A. G.; McNeil, M.; Albersheim, P. *Carbohydr. Res.* **1985**, *138*, 109–126.
- O'Neill, M. A.; Ishi, T.; Albersheim, P.; Darvill, A. G. *Annu. Rev. Plant Physiol. Plant Mol. Biol.* **2004**, *55*, 109–139.
- Ishii, T.; Matsunaga, T. *Carbohydr. Res.* **1996**, *284*, 1–9.





254. Goubet, F.; Council, L. N.; Mohnen, D. *Plant Physiol.* **1998**, *116*, 337–347.
255. Ishikawa, M.; Kuroyama, H.; Takeuchi, Y.; Tsumuraya, Y. *Planta* **2000**, *210*, 782–791.
256. Bourlard, T.; Schaumann-Gaudinet, A.; Bruyant-Vannier, M.-P.; Morvan, C. *Plant Cell Physiol.* **1997**, *38*, 259–267.
257. Kauss, H.; Swanson, A. L. Z. *Naturforsch., B* **1969**, *24*, 28–33.
258. Krupkova, E.; Immerzeel, P.; Pauly, M.; Schmulling, T. *Plant J.* **2007**, *50*, 735–750.
259. Bourlard, T.; Bruyant-Vannier, M.-P.; Schaumann-Gaudinet, A.; Bruyant, P.; Morvan, C. *Sciences de la vie/Life Sci.* **2001**, *324*, 335–343.
260. Goubet, F.; Mohnen, D. *Planta* **1999**, *209*, 112–117.
261. Bouton, S.; Leboeuf, E.; Mouille, G.; Leydecker, M.-T.; Talbotec, J.; Granier, F.; Lahaye, M.; Hofte, H.; Truong, H. N. *Plant Cell* **2002**, *14*, 2577–2590.
262. Ishii, T. *Plant Physiol.* **1997**, *113*, 1265–1272.
263. Whitcombe, A. J.; O'Neill, M. A.; Steffan, W.; Albersheim, P.; Darvill, A. *Carbohydr. Res.* **1995**, *271*, 15–29.
264. Pauly, M.; Scheller, H. V. *Planta* **2000**, *210*, 659–667.
265. Mohnen, D. Biosynthesis of Pectins. In *Pectins: Structure, Function and Manipulation*; Seymour, G. B., Knox, J. P., Eds.; Blackwell Publishing, 2002; pp 52–98.
266. Poon, K. K. H.; Westman, E. L.; Vinogradov, E.; Jin, S.; Lam, J. S. J. *Bacteriol.* **2008**, *190*, 1857–1865.
267. Munoz, R.; Lopez, R.; de Frutos, M.; Garcia, E. *Mol. Microbiol.* **1999**, *31*, 703–713.
268. Saxena, I. M.; Kudlicka, K.; Okuda, K.; Brown, R. M., Jr. *J. Bacteriol.* **1994**, *176*, 5735–5752.
269. Callebaut, I.; Labesse, G.; Durand, P.; Poupon, A.; Canard, L.; Chomilier, J.; Henrissat, B.; Mornon, J.-P. *Cell Mol. Life Sci.* **1997**, *53*, 621–645.
270. Goubet, F.; Morvan, C. *Plant Cell Physiol.* **1993**, *34*, 1297–1303.
271. Brickell, L. S.; Reid, J. S. G. *Prog. Biotechnol.: Pectins Pectinases* **1996**, *14*, 127–134.
272. Geshi, N.; Jorgensen, B.; Scheller, H. V.; Ulvskov, P. *Planta* **2000**, *210*, 622–629.
273. Kato, H.; Tekeuchi, Y.; Tsumuraya, Y.; Hashimoto, Y.; Nakano, H.; Kovac, P. *Planta* **2003**, *217*, 271–282.
274. Konishi, T.; Mitome, T.; Hatsushika, H.; Haque, M. A.; Kotake, T.; Tsumuraya, Y. *Planta* **2004**, *218*, 833–842.
275. Baydoun, E. A.-H.; Abdel-Massih, R.; Dani, D.; Rizk, S. E.; Brett, C. T. J. *Plant Physiol.* **2001**, *158*, 145–150.
276. Baydoun, E. A.-H.; Abdel-Massih, R.; Dani, D.; Rizk, S. E.; Brett, C. T. J. *Plant Physiol.* **2001**, *158*, 145–150.
277. Ishii, T.; Ohnishi-Kameyama, M.; Ono, H. *Planta* **2004**, *219*, 310–318.
278. Peugnet, I.; Goubet, F.; Bruyant-Vannier, M.-P.; Thoirion, B.; Morvan, C.; Schols, H. A.; Voragen, A. J. *Planta* **2001**, *213*, 435–445.
279. Geshi, N.; Pauly, M.; Ulvskov, P. *Physiol. Plant.* **2002**, *114*, 540–548.
280. Abdel-Massih, R.; Baydoun, A.-H.; Brett, C. T. *Planta* **2003**, *216*, 502–511.
281. Konishi, T.; Kotake, T.; Tsumuraya, Y. *Planta* **2007**, *226*, 571–579.
282. Madson, M.; Dunand, C.; Li, X.; Verma, R.; Vanzin, G. F.; Caplan, J.; Shoue, D. A.; Carpita, N. C.; Reiter, W.-D. *Plant Cell* **2003**, *15*, 1662–1670.
283. Bolwell, G. P.; Northcote, D. H. *Biochem. J.* **1983**, *210*, 497–507.
284. Odzuck, W.; Kauss, H. *Phytochemistry* **1972**, *11*, 2489–2494.
285. Rodgers, M. W.; Bolwell, G. P. *Biochemistry* **1992**, *288*, 817–822.
286. Bolwell, G. P.; Northcote, D. H. *Planta* **1981**, *152*, 225–233.
287. Ishii, T.; Ono, H.; Ohnishi-Kameyama, M.; Maeda, I. *Planta* **2005**, *221*, 953–963.
288. Konishi, T.; Ono, H.; Ohnishi-Kameyama, M.; Kaneko, S.; Ishii, T. *Plant Physiol.* **2006**, *141*, 1098–1105.
289. Harholt, J.; Jensen, J. K.; Sorensen, S. O.; Orfila, C.; Pauly, M.; Scheller, H. V. *Plant Physiol.* **2005**, *140*, 49–58.
290. Brown, D. M.; Zeef, L. A. H.; Ellis, J.; Goodacre, R.; Turner, S. R. *Plant Cell* **2005**, *17*, 2281–2295.
291. Persson, S.; Caffall, K. H.; Freshour, G.; Hilley, M. T.; Bauer, S.; Poindexter, P.; Hahn, M.; Mohnen, D.; Somerville, C. *Plant Cell* **2007**, *19*, 237–255.
292. Guillaumie, F.; Sterling, J. D.; Jensen, K. J.; Thomas, O. R. T.; Mohnen, D. *Carbohydr. Res.* **2003**, *338*, 1951–1960.